AD_____

Award Number: W81XWH-10-1-0504

TITLE: A New Therapeutic Strategy for Autosomal Dominant Polycystic Kidney Disease: Activation of AMP Kinase by Metformin

PRINCIPAL INVESTIGATOR: Michael J. Caplan, M.D., Ph.D.

CONTRACTING ORGANIZATION: Yale University
New Haven, CT 06511

REPORT DATE: July 2012

TYPE OF REPORT: Revised Annual

PREPARED FOR: U.S. Army Medical Research and Materiel Command
Fort Detrick, Maryland 21702-5012

REPORT DOCUMENTATION PAGE

Form Approved
OMB No. 0704-0188

1. REPORT DATE *(DD-MM-YYYY)*	2. REPORT TYPE	3. DATES COVERED *(From - To)*
July 2012	Revised Annual	1 July 2011 - 30 June 2012

4. TITLE AND SUBTITLE
A New Therapeutic Strategy for Autosomal Dominant Polycystic Kidney Disease: Activation of AMP Kinase by Metformin

5a. CONTRACT NUMBER

5b. GRANT NUMBER
W81XWH-10-1-0504

5c. PROGRAM ELEMENT NUMBER

6. AUTHOR(S)
Michael J. Caplan, M.D., Ph.D.

E-Mail: michael.caplan@yale.edu

5d. PROJECT NUMBER

5e. TASK NUMBER

5f. WORK UNIT NUMBER

7. PERFORMING ORGANIZATION NAME(S) AND ADDRESS(ES)
Yale University
New Haven, CT 06511

8. PERFORMING ORGANIZATION REPORT NUMBER

9. SPONSORING / MONITORING AGENCY NAME(S) AND ADDRESS(ES)
U.S. Army Medical Research and Materiel Command
Fort Detrick, Maryland 21702-5012

10. SPONSOR/MONITOR'S ACRONYM(S)

11. SPONSOR/MONITOR'S REPORT NUMBER(S)

12. DISTRIBUTION / AVAILABILITY STATEMENT
Approved for Public Release; Distribution Unlimited

13. SUPPLEMENTARY NOTES

14. ABSTRACT

Autosomal dominant polycystic kidney disease is a common inherited disorder. Patients are born with normal kidneys but, over the course of decades, they develop large fluid filled cysts that damage the normal kidney tissue. The damage caused by these cysts can lead ultimately to kidney failure, necessitating kidney transplantation or dialysis. There are currently no approved medications for this condition. Recent research reveals that the formation of cysts is due in part both to inappropriate cell growth and fluid secretion. The enzyme AMPK controls a number of cellular pathways, including those involved in cell growth and fluid secretion. Drugs that activate AMPK, therefore, may constitute an effective therapeutic option for slowing or preventing cyst growth. This research project is aimed at examining the potential of an approved, widely used, inexpensive and low-toxicity drug that can activate AMPK as a potential therapy for the treatment of polycystic kidney disease.

15. SUBJECT TERMS

Autosomal Dominant Polycystic Kidney Disease; Metformin

16. SECURITY CLASSIFICATION OF:			17. LIMITATION OF ABSTRACT	18. NUMBER OF PAGES	19a. NAME OF RESPONSIBLE PERSON
a. REPORT	b. ABSTRACT	c. THIS PAGE			USAMRMC
U	U	U	UU	39	19b. TELEPHONE NUMBER *(include area code)*

Standard Form 298 (Rev. 8-98)
Prescribed by ANSI Std. Z39.18

Yale University

Michael J. Caplan, MD, PHD
CNH Long Professor and Chair
Department of Cellular and
Molecular Physiology
School of Medicine
PO Box 208026
New Haven CT 06520-8026

Campus address:
SHM B116
333 Cedar Street
Telephone: 203 785-7316
Fax: 203 785-4951
Email: michael.caplan@yale.edu

April 4, 2013

Jordan Irvin, Ph.D.
Interdisciplinary Scientific Officer
Congressionally Directed Medical Research Programs
Fort Detrick, MD 21702-5012

Dear Dr. Irvin,

I am very happy to submit a revised version of my 2012 progress report for Department of Defense Peer Reviewed Medical Research Program grant contract number W81XWH-10-1-0504. I apologize that the format and the content of the previous submission were not adequate. I have extensively revised the progress report to ensure that the present version reports on our progress in accomplishing the original Scope of Work. Please feel free to contact me if you have any questions or require any additional information. Thank you very much for you time, patience and consideration.

Sincerely,

Michael Caplan M.D., Ph.D.
C.N.H. Long Professor and Chair

Marybeth Brandi

Marybeth Brandi, Manager
Grant & Contract Administration

Table of Contents

Page

Introduction

Autosomal dominant polycystic kidney disease (ADPKD) is characterized by slow and continuous development of cysts derived from renal tubular epithelial cells. The cysts profoundly alter renal architecture, compressing normal parenchyma and compromising renal function. Nearly half of ADPKD patients ultimately require renal replacement therapy. ADPKD is a common genetic disorder, affecting at least 1 in 1,000 individuals (*1*). There are currently no effective specific clinical therapies for ADPKD. Cystic growth and expansion in ADPKD are thought to result from both fluid secretion into cyst lumens and abnormal proliferation of the cyst-lining epithelium. The rate of fluid secretion into the cyst lumen is directly proportional to the amount of the Cystic Fibrosis Transmembrane Regulator (CFTR) chloride channel in the apical membranes of cyst-lining epithelial cells (*2*). The cells surrounding the cysts manifest increased proliferation (*3, 4*). Mammalian Target of Rapamycin (mTOR) activity is elevated in models of PKD and is likely to be responsible, at least in part, for this hyperproliferative phenotype (*3*). mTOR is a serine/threonine kinase that regulates cell growth and proliferation, as well as transcription and protein synthesis. Interestingly, both the CFTR chloride channel and the mTOR signaling pathway are negatively regulated by the "energy sensing" molecule, Adenosine Monophosphate-activated Protein Kinase (AMPK). AMPK phosphorylates and directly inhibits CFTR, and indirectly antagonizes mTOR through phosphorylation of TSC2 and Raptor (*5-8*). Both of these actions are consistent with the role of AMPK as a regulator that decreases energy-consuming processes such as transport, secretion, and growth when cellular ATP levels are low (*9*). Thus, a drug that activates AMPK might inhibit both the secretory and the proliferative components of cyst expansion. Metformin, a drug in wide clinical use for both non-insulin dependent diabetes mellitus and Polycystic Ovary Syndrome, stimulates AMPK (*10, 11*). We therefore wish to examine whether metformin-induced activation of AMPK can slow cystogenesis through inhibition of mTOR-mediated cellular proliferation and inhibition of CFTR-mediated fluid secretion.

Body

Research Accomplishments Associated with Each Task Outlined in the Approved Statement of Work

Task 1. Characterize the effects of AMPK stimulation on its downstream targets in renal epithelia *in vivo* (months 1-20). The studies encompassed in this task group are designed to determine whether and how AMPK stimulation impacts upon the cellular pathways that are involved in cyst development and expansion. These experiments will make use of cultured MDCK cells and in vitro assays of both AMPK activation and the functional status of AMPK's down-stream targets.

As detailed in the 2011 Progress Report, we have accomplished a substantial portion of the scope of work that was outlined in Tasks 1a, 1b and 1c within the proposed interval. The results of these studies have been published (*12*).

Task 1a. **Establish AMPK stimulation by its pharmacologic activator, metformin in renal epithelial cells *in vitro*.** By immunoblotting for the downstream targets of AMPK, we will confirm that AMPK stimulation has the same effects on its downstream targets in renal epithelia as has been reported in other tissues **(months 1-8)**.

Initially Defined Tasks Largely Completed: See 2011 Progress Report and cited reference #12 for details.

Task 1b. **Characterize the physiological consequences of inhibition of AMPK downstream target CFTR.** This will be accomplished via short circuit current measurements performed on MDCK cells transfected to express CFTR and grown on permeable filter supports **(months 6-16)**.

Initially Defined Tasks Largely Completed: See 2011 Progress Report and cited reference #12 for details.

Task 1c. **Assess AMPK-mediated mTOR inhibition.** This will be accomplished both by direct assay of the phosphorylation status of downstream mTOR targets and by determining the physiological implications of this inhibition through measurements of cell proliferation **(months 10-20)**.

Initially Defined Tasks Largely Completed: See 2011 Progress Report and cited reference #12 for details.

Planned Studies for Task 1 (from 2011 Progress Report): We will assess the extent to which varied dosing regimens can produce AMPK activation in wild type mice. In addition, we will determine whether activation of AMPK by metformin treatment exhibits any isoform preference. To test this possibility, we will measure activation of renal AMPK by metformin using antibodies that

will allow us to distinguish between the α1 or α2 isoforms of the AMPK α-subunit. In addition, we will assess the effects of AMPK activation on the distribution and activity of renal CFTR in vivo in mice treated with metformin. Finally, we will determine whether the metformin dosing regimen that is optimal for achieving AMPK activation is also optimal for producing mTOR inhibition by using antibodies directed against p4E-BP1 to assess the level of mTOR activation in kidney tissue derived from treated animals.

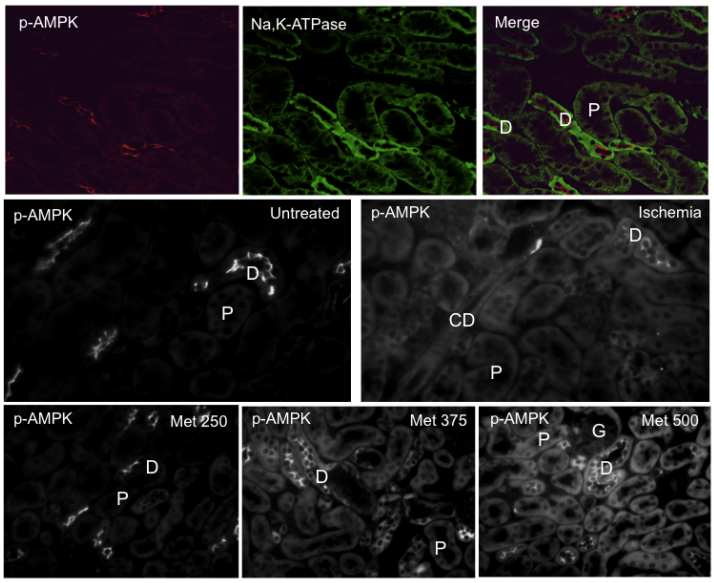

Figure 1: Immunocytochemical assessment of AMPK activation in mouse kidneys in situ. AMPK activation levels were assessed by staining sections with an antibody directed against p-AMPK. We find that treatment with 375 mg/kg produces levels of AMPK activation that are comparable to those produced by renal ischemia.

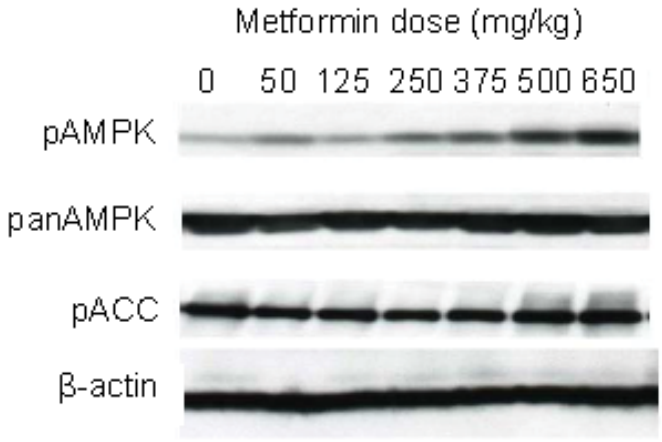

Figure 2: Western blot analysis of tissue prepared from snap-frozen kidneys from metformin-treated mice. AMPK activation was assessed by blotting for p-AMPK. Treatment with metformin produces dose-dependent activation of AMPK.

Progress on Planned Studies for Task 1:

Identification of Dosing Regimens that Produce AMPK Activation in Wild Type Mice

We measured the effects of varying doses of metformin on AMPK activity in mice *in vivo*. This analysis was performed by immunocytochemistry and by western blotting. In both cases, ischemic injury was used as a positive control to produce maximal AMPK activation. AMPK is activated in response to energy deprivation, which results in the accumulation of high cytosolic levels of the enzyme's allosteric activator AMP. Renal ischemia produces energy deprivation in renal tubules and is a powerful stimulus leading to the activation of AMPK in the kidney. The localization of activated, phosphorylated form of AMPK (p-AMPK) at baseline and after acute kidney ischemia has been characterized in the rat (*13, 14*). In murine kidneys, we demonstrate similar localization of p-AMPK under these conditions. Upon immunofluorescence staining using a p-AMPK-specific antibody, p-AMPK was detected in the apical membranes of distal tubules of mice at baseline. Following ischemia, there was a diffuse increase in p-AMPK fluorescence globally, including within proximal tubules and glomeruli (Fig. 1). Metformin has been demonstrated to activate AMPK in the heart, vascular tissue, and kidney

homogenates (*15-17*). We observed that treatment with metformin delivered by IP injection results in increased fluorescence of p-AMPK in all cortical tubule segments (Fig. 1). Furthermore, this activation appears to be dose-dependent, as assessed by immunofluoresence microscopy. Western blot analysis to measure p-AMPK levels was also performed on renal tissue that was snap-frozen in situ using a specially designed forceps that had been pre-cooled in liquid nitrogen. This method also confirmed that AMPK activation occurs in response to increasing metformin doses (Figure 2). The data suggest that the metformin dose that has been used in our in vivo studies (*12*) produces reproducible AMPK activation in situ (Figure 3). Our efforts to assess the isoform specificity of AMPK activation *in vivo* are on-going, as are our efforts to determine the effects of AMPK activation on CFTR distribution and mTOR activity in kidneys *in vivo*.

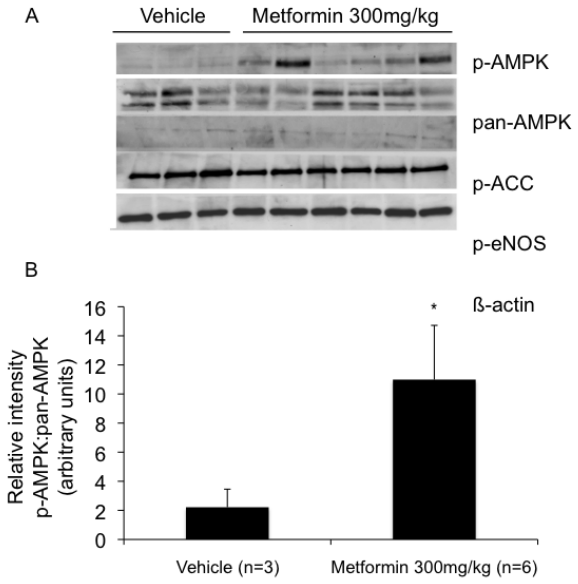

Figure 3: **Figure 2: Western blot analysis of tissue prepared from snap-frozen kidneys from metformin-treated mice.** Treatment *in vivo* results in reproducible activation of renal AMPK.

Additional Task 1a, b and c-related Research Accomplishments 2011-2012:

1. **Further investigation of metformin's mode of action.**

Very recent published data suggests that the mechanism of action of metformin *in vivo* may involve pathways other than those related to AMPK (*18*). It is critically important to determine whether the potential therapeutic effects of metformin that we have identified in the context of Autosomal Dominant Polycystic Kidney Disease are due to its capacity to activate AMPK or are instead due to its effects on other targets. Recent research indicates that metformin can decrease cellular levels of cAMP (*18*). This is especially relevant in the setting of Autosomal Dominant Polycystic Kidney Disease because a substantial body of research has demonstrated that elevation of cAMP promotes cyst growth *in vitro* and *in vivo* (*19, 20*). Furthermore, drug therapies that reduce cAMP slow cyst growth both in mouse models of Autosomal Dominant Polycystic Kidney Disease (*21*) as well as in human Autosomal Dominant Polycystic Kidney Disease patients (*22*). To begin to explore this possibility, we have undertaken to assess the effects of other AMPK activators. These include AICAR, the A-769662 compound from Abbott Laboratories, and two new AMPK activating compounds provided to us by Glaxo Smith Kline on an investigational basis. We have begun to assess whether these compounds modulate cystic growth of renal epithelial cells maintained in three dimensional culture conditions. If this proves to be the case we will conclude that AMPK is indeed a pharmacological target of value in Autosomal Dominant Polycystic Kidney Disease and that the therapeutic potentials of novel compounds that activate AMPK should be explored in relevant tissue culture and animal models. We have demonstrated that these compounds activate AMPK in cells in culture. We have now undertaken dose response analyses to determine the optimal concentrations and time courses for activating AMPK in renal epithelial cells in culture

(see Figure 4). Once identified, these conditions will be applied in experiments designed to assess the effects of these compounds on the cystic growth of renal epithelial cells maintained in three dimensional culture.

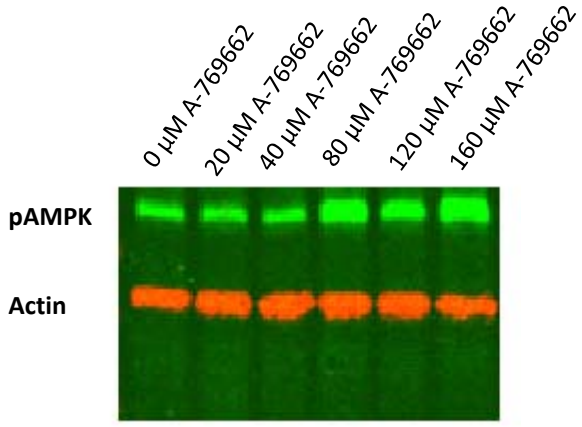

Figure 4: Dose response analysis of AMPK activation by A-769662 in cultured MDCK renal epithelial cells.

2. Exploration of a novel mechanism that may connect AMPK inhibition to the development of Autosomal Dominant Polycystic Kidney Disease.

A poster presented at last year's American Society of Nephrology meeting, from the laboratory of Dr. Alessandra Boletta, reported that cells homozygous for ADPKD-causing mutations manifest substantial perturbations in energy production (Rowe, I. et al. JASN 23:1A, 2012). These cells exhibit very high levels of glycolysis and low levels of oxidative metabolism, reminiscent of the Warburg effect that is seen in tumor cells. As a result of the very high levels of glycolysis the cytoplasmic levels of ATP are very high and levels of active AMPK are consequently very low. These data lend further support to the idea that small molecule AMPK-activators may have therapeutic benefit in ADPKD. Very recently, we have explored the mechanisms responsible for the "Warburg-like" excessive glycolytic activity that is observed in ADPKD cells. We have identified a key enzyme that is involved in regulating energy synthesis to be another potential drug target in ADPKD.

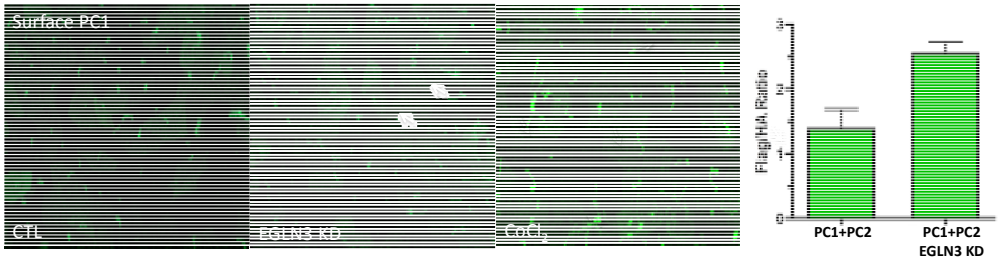

Fig. 5: EGLN3 KD induces an increase in surface PC1 in polarized LLCPK cells: Left 3 panels: surface IF using Flag antibody; Right panel: fluorescence plate reader analysis measuring ratio of Flag (surface) to HA (total) signal

One of the key steps in the regulation of the tricarboxylic acid cycle and aerobic metabolism is the production of acetyl CoA from pyruvate by pyruvate dehydrogenase (PDH) (*23*). PDH is subjected to inhibitory phosphorylation by PDH kinase, and this inhibition is reversed by a calcium-activated PDH phosphatase. Polycystin-2 can function as an ER calcium release channel (*24*), and calcium release from the ER stimulates aerobic metabolism by activating PDH phosphatase and thus PDH (*25*). The channel activity of TRPA1, which like polycystin-2 is a member of the TRP family, is directly regulated by oxygen through the oxidation and hydroxylation of specific cysteine and proline residues, respectively (*26*). This prolyl hydroxylation is mediated by prolyl hydroxylase domain containing (PHD) enzymes, which are critical sensors of changes in oxygen levels (*27, 28*). We have found through mass spectrometric analysis that polycystin-1 and polycystin-2 are both modified by cysteine oxidation and prolyl hydroxylation at highly conserved

sites. Furthermore, we have found that the polycystin 1/2 complex associates with a PHD enzyme called EGLN3, and that reducing the expression or activity of EGLN3 substantially alters polycystin 1/2 behavior.

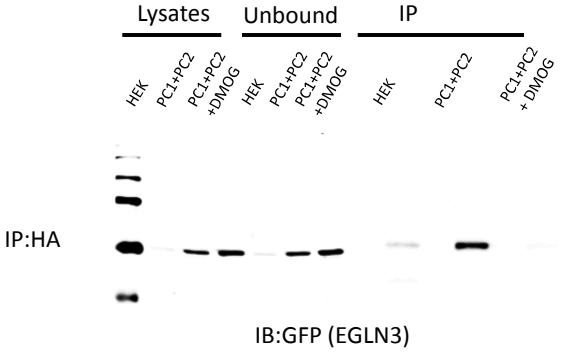

Fig. 6 EGLN3 Co-IPs with HA-tagged PC1, and this Co-IP is blocked by EGLN3 inhibitor DMOG

We find that shRNA-mediated knockdown of EGLN3, which is also known as prolyl hydroxylase domain containing protein 3 (PHD3), leads to increased surface expression of PC1 (Figure 5). As noted above, the PHD proteins are cellular O_2 sensors and regulate the cell's hypoxia response pathway. In the presence of O_2, PHD proteins hydroxylate proline residues on the hypoxia induced factor HIF1α and this modification targets HIF1α for degradation (*27*). PHD modification of TRPA1 contributes to the O_2-sensitivity of TRPA1 channel gating and also modulates its cell surface expression (*26*). The O_2-sensitivity of TRPA1 gating also involves direct non-enzymatic oxidation of TRPA1 cysteine residues. We find that knockdown of EGLN3 expression or inhibition of EGLN3 activity (using CoCl2) in LLC-PK1 cells stably expressing polycystin-1 and polycystin-2 led to a substantial increase in the quantity of polycystin-1 present in the apical plasma membrane (Fig. 5). Mass spectrometric analysis of polycystin-1 and polycystin-2 purified from transfected cells by immunoprecipitation reveals the presence of several hydroxylated proline residues and oxidized cysteine residues. The oxidized cysteines reside in close proximity to the hydroxylated prolines, and several of these residues are found in sequence motifs that resemble the PHD target site in TRPA1. EGLN3 co-immunoprecipitates with PC1, and this association is prevented by inhibiting EGLN3 with DMOG (Figure 6). Taken together, these data support the exciting hypothesis that the trafficking and channel activity of the polycystin-1/2 complex is modulated by PHD proteins in response to changes in cellular O_2 levels. These findings further suggest a novel hypothesis that accounts for the metabolic perturbations that accompany the loss of polycystin 1 expression and the potential therapeutic utility of metformin. We propose that oxygen levels regulate the calcium channel activity of the polycystin 1/2 complex, which in turn regulates oxidative metabolism by mediating the release of calcium from the ER, leading to activation of PDH-phosphatase and hence of PDH.

Planned Studies for Task 1

We will continue our assessment of the potential efficacy of other AMPK activators, including AICAR, A-769662 and the two compounds from Glaxo Smith Kline. We will identify the dosing regimens required to produce AMPK activation for each of these compounds in renal epithelial cells in culture. These studies will use MDCK canine renal epithelial cells. They will also use a mouse cell line with a *Pkd1*$^{-/-}$ genotype (*29*). These cells form cysts when grown in three dimensional culture conditions, whereas a closely related cell line with a *Pkd1*$^{+/-}$ genotypes forms tubules when cultivated in the same culture conditions (*30*). Once optimal AMPK-activating doses for each compound have been established we will assess the effects of these compounds on cell proliferation, apoptosis and mTOR activation. Both cell proliferation and apoptosis will be assessed by immunofluorescence microscopy. Cell proliferation will be determined by using an anti-BrdU

antibody to measure BrdU incorporation. Apoptosis will be determined by using an antibody directed against cleaved caspase 3. These experiments will be performed using MDCK cells and the mouse *Pkd1*$^{-/-}$ and *Pkd1*$^{+/-}$ cell lines. We will also assess the extent to which these AMPK-activating compounds alter the morphogenesis of these cell lines grown in three dimensional culture conditions. As noted above, the *Pkd1*$^{-/-}$ cells form cysts when cultivated in three dimensional culture conditions, whereas the heterozygous *Pkd1*$^{+/-}$ cells form tubule-like structures in this setting. We will determine whether metformin, AICAR, A-769662 and the compounds from Glaxo Smith Kline induce the *Pkd1*$^{-/-}$ cells to form tubule-like structures when they are administered in AMPK-activating doses.

Task 2. Evaluate the *in vitro* and *in vivo* effects of metformin-induced AMPK inhibition of mTOR and CFTR in the context of *in vitro* and *in vivo* models of cystic kidney disease (months 12-36).

Task 2a. **Determine the effect of metformin treatment on average cyst size and cyst number using *in vitro* models of cystogenesis.** These experiments will be performed with renal epithelial cells that spontaneously form cysts when suspended in a collagen matrix. Cyst size and number will be determined by quantitative fluorescence microscopy techniques **(months 12-24)**.

Initially Defined Task Largely Completed: See 2011 Progress Report and cited reference #12 for details.

Task 2b. **Perform an *in vivo* trial of metformin treatment on Ksp-Cre, Pkd1$^{flox/-}$ mice.** This mouse model represents a very severe model of ADPKD. These experiments will permit the potential for metformin therapy to slow disease progression to be evaluated in mice that have developed cystic disease prior to the initiation of treatment **(months 12-28)**. These experiments will utilize 75 mice, 25 of which will be used in months 1-12 for breeding purposes, to generate a stable colony of 50 mice with the required genotypes that will be used in the experiments associated with this task.

Initially Defined Task Largely Completed: See 2011 Progress Report and cited reference #12 for details.

Task 2c. **Evaluate the effect of metformin in a mouse model of inducible PKD.** We will use an inducible mouse model of PKD (pCAGGS-cre, tamoxifen-activatable Pkd1$^{flox/-}$ mice), which will allow mice to be pre-treated with metformin prior to disease induction. This will allow us to gauge the therapeutic benefit of metformin under conditions that may more accurately mimic at least certain aspects of the progression of the human disease **(months 20-36)**. These experiments will utilize 75 mice, 25 of which will be used in months 1-12 for breeding purposes, to generate a stable colony of 50 mice with the required genotypes that will be used in the experiments associated with this task.

Initially Defined Task Largely Completed: See 2011 Progress Report and cited reference #12 for details.

Planned Studies for Task 2 (from 2011 Progress Report): The studies outlined in the Planned Studies for Task 1 will identify a metformin dosing regimen that is optimal for achieving activation of renal AMPK. We will test the efficacy of this regimen in preventing or slowing cystogenesis in two mouse models of autosomal dominant polycystic kidney disease. We will cross the mice carrying a $Pkd1^{flox/-}$ genotype with mice expressing Cre under the Ksp-cadherin or the Pkhd1 promoters to generate rapidly and slowly progressive models of the disease, respectively. To assess the effects of optimal metformin treatment on cystogenesis in these animals we will measure kidney weight to body weight ratios, cystic indices, and plasma levels of BUN and creatinine. We are initiating a collaboration with an investigator who has generated conditional knockout mouse models of AMPK α1 and α2 isoform expression. When these models become available (and once approval has been granted for the relevant modifications of the ACURO animal use appendix and our IACUC animal use protocol) we will cross the AMPK α1 and α2 null alleles into homozygous and heterozygous $Pkd1^{flox/-}$ backgrounds. We anticipate that absence of expression of one or the other AMPK subunits exacerbates the progression of the disease and reduces the efficacy of metformin treatment.

Progress on Planned Studies for Task 2: We continue our efforts towards identifying an optimal metformin dosing regimen. We are exploring variations dose size, dose frequency and route of delivery. Our end point for assessment of dose efficacy continues to be measurement of AMPK activation *in situ* using an antibody directed against phospho AMPK in both immunofluorescence and western blot experiments (for examples of this type of analysis see Figures 1,2 and 3). We have obtained AMPK $\alpha1^{flox/flox}$ mice as well as AMPK $\alpha2^{-/-}$ mice. We are currently in the process of crossing these mice to generate AMPK $\alpha1^{flox/flox}$; AMPK $\alpha2^{-/-}$ mice. We are also crossing the resultant animals with mice that express Cre under the control of the distal tubule-specific Ksp cadherin promoter. Once these mice are produced in adequate quantities we will cross them with the $Pkd1^{flox/flox}$ mice that we used in our previous efficacy experiments (*12*). The complexity of the requisite breeding schemes has delayed the production of these mice somewhat beyond our original projections, but this effort is now well underway.

Additional Task 2a, b and c-related Research Accomplishments 2011-2012

1. **Identification of a novel small molecule approach to correcting the perturbation in energy metabolism that is associated with Autosomal Dominant Polycystic Kidney Disease**

As noted above, we hypothesize that AMPK activity may be reduced in the context of Autosomal Dominant Polycystic Kidney Disease due to the inappropriate acceleration of glycolytic activity, resulting in high levels of ATP and reduced levels of AMP. The reduced AMPK activity could contribute to the pathogenesis of Autosomal Dominant Polycystic Kidney Disease by de-repressing mTOR and CFTR activities. Thus, correcting the perturbation in energy metabolism could potentially help to correct the reduction in AMPK activity and with it the Autosomal Dominant Polycystic Kidney Disease pathological phenotype. Pyruvate dehydrogenase is inhibited via a phosphorylation event that is mediated by pyruvate dehydrogenase kinase. Dichloroacetic acid (DCA) is a very well characterized inhibitor of pyruvate dehydrogenase kinase (*31*). Administration of DCA stimulates the tricarboxylic acid cycle and aerobic metabolism. Furthermore, DCA has

been used in human clinical trials designed to test its therapeutic potential in the setting of congenital lactic acidosis and also in the setting of cancer. Taking advantage of a 3-dimensional culture in vitro cyst growth assay that we have used extensively in our laboratory, we find that treatment with DCA dramatically inhibits cyst formation by ADPKD cells, and instead induces them to grow into tubule-like structures (see Figure 7). Thus, we believe that the enzyme that we have identified constitutes another extremely interesting target for ADPKD drug development.

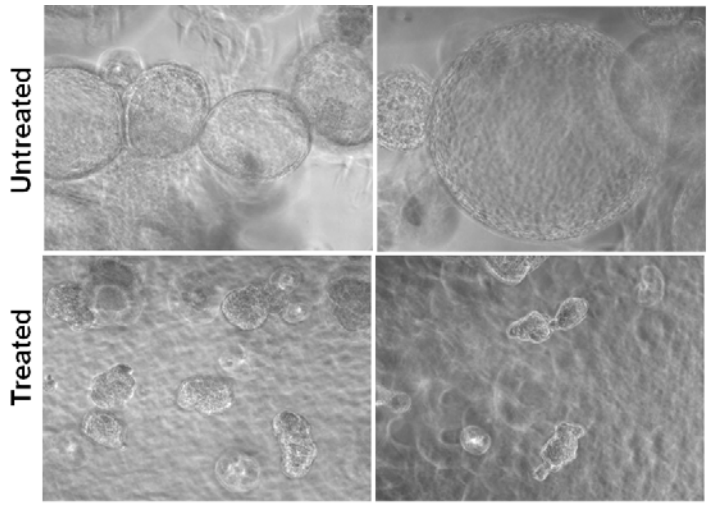

Figure 7: Treatment with DCA, which modulates mitochondrial energy metabolism, substantially reduces cyst development when *Pkd1*$^{-/-}$ cells are grown in 3D culture.

Planned Studies for Task 2

We will continue our experiments designed to identify the optimal metformin dosing regimen. Once this work has been completed we will apply this regimen to mice carrying a *Pkd1*$^{flox/-}$ genotype and that express Cre under the Ksp-cadherin or the Pkhd1 promoters, which constitute rapidly and slowly progressive models of the disease, respectively. To assess the effects of optimal metformin treatment on cystogenesis in these animals we will measure kidney weight to body weight ratios, cystic indices, and plasma levels of BUN and creatinine. We will continue our efforts to produce AMPK $\alpha1^{flox/flox}$; AMPK $\alpha2^{-/-}$ mice and to generate mice that carry this genotype on a *Pkd1*$^{flox/-}$ background. Once these mice have been produced we will monitor the progression of renal cyst development in these animals to determine whether the absence of AMPK expression produces more severe or rapidly progressing disease. We will also subject these animals to metformin treatment in order to determine whether the response to metformin treatment requires the presence of AMPK activity. Finally, we will continue our experiments with DCA using *Pkd1*$^{-/-}$ cells grown in three dimensional culture. The goal of these experiments will be to identify and optimal DCA dosing regimen that reduces the number or rate of expansion of cystic structures. Both cell proliferation and apoptosis will be assessed by immunofluorescence microscopy. Cell proliferation will be determined by using an anti-BrdU antibody to measure BrdU incorporation. Apoptosis will be determined by using an antibody directed against cleaved caspase 3. We will also assess whether this concentration of DCA alters the phosphorylation status of PDH and of AMPK.

Key Research Accomplishments

- Metformin stimulates AMPK in mice *in vivo*.
- A-769662 stimulates AMPK in MDCK cells in culture.
- Polycystin trafficking is modulated by prolylhydroxylase domain containing proteins.
- Prolylhydroxylase domain containing proteins interact physically with polycystins.
- Inhibition of pyruvate dehydrogenase kinase with DCA slows cystogenesis in *in vitro* three dimensional culture models.

Reportable Outcomes

- Peer reviewed primary data publication:

  Merrick, D.M., H.C. Chapin, Z. Yu, S. Somlo, J. Hogenesch, and M.J. Caplan The γ-secretase cleavage product of Polycystin-1 regulates Tcf and CHOP-mediated transcriptional activation through a p300-dependent mechanism. Dev. Cell, 22, 197–210, 2012.

- Invited review articles:

  Pluznick J.L. and M.J. Caplan. Novel sensory signaling systems in the kidney. Curr. Opin. Nephrol. Hypertens. 21:404-409, 2012.

(Please note—all of the journals in which publications supported by the present award have appeared will be contacted in order to ensure that the acknowledgment appropriately references Department of Defense Peer Reviewed Medical Research Program and the grant contract number (W81XWH-10-1-0504))

Conclusion

AMPK activity can be pharmacologically targeted with metformin to reduce the growth of renal cysts. Metformin acts through AMPK to decrease both epithelial fluid secretion by directly inhibiting CFTR, and to decrease cellular proliferation by indirectly targeting mTOR. Metformin stimulates AMPK phosphorylation in cultured MDCK renal epithelial cells, and this phosphorylation correlates with increased AMPK activity, as evidenced by an increase in the level of the AMPK-mediated inhibitory phosphorylation of ACC. Metformin's inhibitory action on CFTR-mediated chloride transport is AMPK-dependent. Additionally, we have shown that metformin inhibition of mTOR translates into an AMPK-dependent inhibition of cell proliferation. Using both an in vitro model of MDCK cell cystogenesis as well as embryonic kidneys ex vivo, we have demonstrated that metformin decreases cyst size, and fractional cyst area, respectively. Finally, we illustrated the potential therapeutic utility of metformin by testing it in two murine models of ADPKD, both of which are attributable to inactivation of the gene encoding polycystin-1.

In this study, only one dose known to activate AMPK in vivo was tested. When considered on a simple mg/kg basis, this dose appears considerably higher than the current maximum dose prescribed for patients with diabetes or Polycystic Ovary Syndrome. However, human equivalent dose extrapolation is more accurately calculated based on body surface area than on weight. When this calculation is performed for a 60 kg adult, the dose used in our mouse studies extrapolates to a daily dose of approximately 1500 mg, which falls well within the range in which metformin is safely used in humans. It is likely, based on the established pharmacokinetics of metformin, that single daily dosing is suboptimal, and thus we are almost certainly not observing the maximal suppressive effects that metformin could potentially exert on the severity of cyst growth.(44) Support for this contention derives from the data presented in Figure 4c, since in the embryonic kidney model, cyst growth rapidly resumes shortly after removal of metformin from the culture media. Thus, short term intermittent metformin exposure may not be adequate to optimally suppress cyst development. It is quite possible that even lower doses administered more frequently might produce beneficial effects in the setting of polycystic kidney disease. It is important to note that our efforts to assess effects of metformin treatment on renal functional parameters such as serum concentrations of BUN and creatinine were inconclusive, due in part to a large degree of inter-individual variability. Further studies, perhaps employing more slowly progressive disease models, will be required to reduce this variance and to assess the extent to which metformin treatment can protect or improve renal function in the setting of polycystic kidney disease. In addition, subsequent development of metformin for this clinical application will require pharmacokinetic and pharmacodynamic studies designed to identify an ideal dosing regimen that achieves maximal activation of renal tubular AMPK. We are now working to optimize the metformin dosing regimen to ensure that it produces the most substantial and longest lasting activation of AMPK possible. These new dosing regimens will be tested in the relevant mouse models of Autosomal Dominant Polycystic Kidney Disease.

Finally, we have made a novel discovery that may explain the recent observation that energy metabolism is perturbed in kidney cells that lack the expression of polycystin-1. We have found that the polycystins interact with and are regulated by prolylhydroxylase domain containing proteins. Thus, the polycystins may serve as components of cellular oxygen sensors. Furthermore, the calcium channel activity of the polycystins may regulate metabolism by controlling the calcium-sensitive pyruvate dehydrogenase phosphatase, which in turn activates pyruvate dehydrogenase. In fact, stimulating pyruvate dehydrogenase activity with DCA ameliorates aspects of the cystic phenotype of renal epithelial cells grown in three dimensional culture. Thus, our data suggest a new

comprehensive mechanism that accounts for the perturbations in energy metabolism that are detected in Autsomal Dominant Polycystic Kidney Disease. Furthermore, these data explain the potential therapeutic utility of AMPK activation in this context and also suggest exciting new therapeutic modalities.

So What?

Metformin is taken by millions of Americans each year. It is currently FDA-approved for the treatment of Non-Insulin Dependent Diabetes (Type II DM) and, intriguingly, for Polycystic Ovary Syndrome, a disease that shares a name similar to that of Polycystic Kidney Disease but whose pathogenesis is even less well understood. In fact, metformin is often considered first line therapy for the treatment of Type II DM, due to its relatively small side effect profile. Recent literature suggests that metformin's activation of AMPK may be due to its ability to prevent AMP breakdown, although the exact mechanisms of action of metformin in Polycystic Ovary Syndrome or in Type II DM remain largely unknown. Recent reports also suggest that metformin may exert an anti-neoplastic effect. It has been reported that metformin acts in a dose-dependent manner to inhibit the proliferation of breast cancer cells and that this effect can be blocked in the presence of small interfering RNA directed against AMPK. This inhibition is also associated with a decrease in mTOR activation, suggesting that metformin's anti-proliferative effect is directed through the activation of AMPK, and consequent inhibition of mTOR.

There are numerous therapies for ADPKD in development or in clinical trials, including vasopressin receptor inhibitors, calcium sensing receptor inhibitors, CFTR-inhibitors, cell cycle inhibitors, and rapamycin. Each of these strategies targets one or the other of the key processes (proliferation and secretion) thought to be involved in the pathogenesis of PKD. By acting through AMPK, metformin may offer the significant advantage of blocking both (SI 4). Moreover, metformin is already FDA approved and generally well-tolerated. The most serious, albeit rare, side effect of metformin is lactic acidosis and, since metformin is cleared by the kidney, chronic renal disease has been considered to be a potential predisposing factor for this complication. However, metformin use could ideally be initiated at an early stage in ADPKD progression, prior to the development of substantial cyst burden and compromise of renal function, thus allowing for maximal preventive benefit and minimizing the potential for renal dysfunction to limit the safe use of the drug. Given the relatively late onset and slow progression of ADPKD it is conceivable that, even if metformin were to have only modest effects in delaying or slowing cyst development, it might significantly increase the time to the development of end stage renal disease and perhaps reduce the need for renal replacement therapy.

We find that metformin stimulates AMPK, resulting in inhibition of both CFTR and mTOR, and thereby, both epithelial secretion and proliferation, respectively. Our data suggest the possible utility of metformin as a therapy for ADPKD and that AMPK is a novel potential pharmacological target for ADPKD therapy. The large body of knowledge associated with metformin administration could conceivably facilitate the translation of these findings into clinical trials to test the proposition that metformin is a safe and promising approach that exploits AMPK activity to treat this challenging disease.

References

1. V. E. Torres, P. C. Harris, Y. Pirson, *Lancet* **369**, 1287 (Apr 14, 2007).
2. C. J. Davidow, R. L. Maser, L. A. Rome, J. P. Calvet, J. J. Grantham, *Kidney Int* **50**, 208 (Jul, 1996).
3. P. R. Wahl *et al.*, *Nephrol Dial Transplant* **21**, 598 (Mar, 2006).
4. S. Shibazaki *et al.*, *Hum Mol Genet* **17**, 1505 (Jun, 2008).
5. K. R. Hallows, V. Raghuram, B. E. Kemp, L. A. Witters, J. K. Foskett, *J Clin Invest* **105**, 1711 (Jun, 2000).
6. J. D. King, Jr. *et al.*, *Am J Physiol Cell Physiol* **297**, C94 (Jul, 2009).
7. D. M. Gwinn *et al.*, *Mol Cell* **30**, 214 (Apr 25, 2008).
8. K. Inoki, T. Zhu, K. L. Guan, *Cell* **115**, 577 (Nov 26, 2003).
9. D. G. Hardie, *Nat Rev Mol Cell Biol*, (Aug 22, 2007).
10. G. Zhou *et al.*, *J Clin Invest* **108**, 1167 (Oct, 2001).
11. R. J. Shaw *et al.*, *Science* **310**, 1642 (Dec 9, 2005).
12. V. Takiar *et al.*, *Proc Natl Acad Sci U S A* **108**, 2462 (Feb 8, 2011).
13. P. F. Mount *et al.*, *Am J Physiol Renal Physiol* **289**, F1103 (Nov, 2005).
14. S. Fraser *et al.*, *Am J Physiol Renal Physiol* **288**, F578 (Mar, 2005).
15. M. J. Lee *et al.*, *Am J Physiol Renal Physiol* **292**, F617 (Feb, 2007).
16. L. Solskov *et al.*, *Basic Clin Pharmacol Toxicol* **103**, 82 (Jul, 2008).
17. M. H. Zou *et al.*, *J Biol Chem* **279**, 43940 (Oct 15, 2004).
18. R. A. Miller *et al.*, *Nature* **494**, 256 (Feb 14, 2013).
19. T. Yamaguchi *et al.*, *J Biol Chem* **279**, 40419 (Sep 24, 2004).
20. H. C. Chapin, M. J. Caplan, *J Cell Biol* **191**, 701 (Nov 15, 2010).
21. V. H. Gattone, 2nd, X. Wang, P. C. Harris, V. E. Torres, *Nat Med* **9**, 1323 (Oct, 2003).
22. V. E. Torres *et al.*, *N Engl J Med* **367**, 2407 (Dec 20, 2012).
23. M. G. Vander Heiden, L. C. Cantley, C. B. Thompson, *Science* **324**, 1029 (May 22, 2009).
24. P. Koulen *et al.*, *Nat Cell Biol* **4**, 191 (Mar, 2002).
25. C. Cardenas *et al.*, *Cell* **142**, 270 (Jul 23, 2010).
26. N. Takahashi *et al.*, *Nat Chem Biol* **7**, 701 (Oct, 2011).
27. P. Jaakkola *et al.*, *Science* **292**, 468 (Apr 20, 2001).
28. C. J. Schofield, P. J. Ratcliffe, *Nat Rev Mol Cell Biol* **5**, 343 (May, 2004).
29. D. Joly *et al.*, *J Biol Chem* **281**, 26329 (Sep 8, 2006).
30. D. Merrick *et al.*, *Dev Cell* **22**, 197 (Jan 17, 2012).
31. E. D. Michelakis, L. Webster, J. R. Mackey, *Br J Cancer* **99**, 989 (Oct 7, 2008).

Appendix

Reprints of:

Merrick, D.M., H.C. Chapin, Z. Yu, S. Somlo, J. Hogenesch, and M.J. Caplan The γ-secretase cleavage product of Polycystin-1 regulates Tcf and CHOP-mediated transcriptional activation through a p300-dependent mechanism. Dev. Cell, 22, 197–210, 2012.

Pluznick J.L. and M.J. Caplan. Novel sensory signaling systems in the kidney. Curr. Opin. Nephrol. Hypertens. 21:404-409, 2012.

Developmental Cell
Article

The γ-Secretase Cleavage Product of Polycystin-1 Regulates TCF and CHOP-Mediated Transcriptional Activation through a p300-Dependent Mechanism

David Merrick,[1,2] Hannah Chapin,[1,2] Julie E. Baggs,[5] Zhiheng Yu,[3] Stefan Somlo,[3,4] Zhaoxia Sun,[4] John B. Hogenesch,[5] and Michael J. Caplan[1,2,*]
[1]Department of Cellular and Molecular Physiology
[2]Department of Cell Biology
[3]Department of Medicine, Section of Nephrology
[4]Department of Genetics
Yale University School of Medicine, New Haven, CT 06510, USA
[5]Department of Pharmacology, Institute of Translational Medicine and Therapeutics, Penn Genome Frontiers Institute, University of Pennsylvania School of Medicine, Philadelphia, PA 19104-6145, USA
*Correspondence: michael.caplan@yale.edu
DOI 10.1016/j.devcel.2011.10.028

SUMMARY

Mutations in *Pkd1*, encoding polycystin-1 (PC1), cause autosomal-dominant polycystic kidney disease (ADPKD). We show that the carboxy-terminal tail (CTT) of PC1 is released by γ-secretase-mediated cleavage and regulates the Wnt and CHOP pathways by binding the transcription factors TCF and CHOP, disrupting their interaction with the common transcriptional coactivator p300. Loss of PC1 causes increased proliferation and apoptosis, while reintroducing PC1-CTT into cultured *Pkd1* null cells reestablishes normal growth rate, suppresses apoptosis, and prevents cyst formation. Inhibition of γ-secretase activity impairs the ability of PC1 to suppress growth and apoptosis and leads to cyst formation in cultured renal epithelial cells. Expression of the PC1-CTT is sufficient to rescue the dorsal body curvature phenotype in zebrafish embryos resulting from either γ-secretase inhibition or suppression of *Pkd1* expression. Thus, γ-secretase-dependent release of the PC1-CTT creates a protein fragment whose expression is sufficient to suppress ADPKD-related phenotypes in vitro and in vivo.

INTRODUCTION

Autosomal-dominant polycystic kidney disease (ADPKD), a common genetic disorder, produces fluid-filled renal cysts that disrupt the normal tubular architecture and can ultimately lead to kidney failure (Wilson, 2004). Most cases (85%) result from mutations in the gene encoding polycystin-1 (*Pkd1*), with the remaining 15% resulting from mutations in the gene encoding polycystin-2 (*Pkd2*) (Harris and Torres, 2009; Rossetti et al., 2007). Polycystin-1 (PC1) has a large extracellular domain, 11 transmembrane spans, and a short carboxy-terminal cytoplasmic tail (Hughes et al., 1995). The PC1 C-terminal tail (PC1-CTT) has been implicated in the regulation of several signaling pathways, including Wnt (Kim et al., 1999; Lal et al., 2008; Zhang et al., 2007), mTOR (Shillingford et al., 2006), p21/JAK/STAT (Bhunia et al., 2002; Low et al., 2006; Talbot et al., 2011), and activator protein-1 (Arnould et al., 1998; Chauvet et al., 2004; Parnell et al., 2002). Polycystin-2 is a nonselective calcium-permeable cation channel that interacts and forms a complex with PC1 via the coiled-coil domains present in each of these proteins (Qian et al., 1997).

PC1 is subject to several proteolytic cleavages (Chapin and Caplan, 2010; Woodward et al., 2010), including an autocatalytic event that releases the N-terminal extracellular domain, which remains noncovalently associated with the transmembrane domains (Qian et al., 2002). The PC1-CTT is cleaved and translocates to the nucleus (Bertuccio et al., 2009; Chauvet et al., 2004; Low et al., 2006; Talbot et al., 2011). Nuclear PC1-CTT regulates cell-signaling pathways, including activation of STAT6/P100 and STAT3 (Low et al., 2006; Talbot et al., 2011), and inhibition of β-catenin-mediated canonical Wnt signaling (Lal et al., 2008). ADPKD cyst formation is thought to occur, at least in part, as a result of dysregulation of epithelial cell proliferation and of apoptosis (Chapin and Caplan, 2010; Lanoix et al., 1996; Shibazaki et al., 2008; Starremans et al., 2008; Takiar and Caplan, 2011).

We show that the CTT of PC1 is released by a γ-secretase-dependent cleavage and translocates to the nucleus, where it regulates transcriptional pathways involved in proliferation and apoptosis. Expression of the CTT fragment corrects several of the growth and morphogenesis-related phenotypes that characterize *Pkd1* null cells grown in three-dimensional (3D) culture. Furthermore, expression of the PC1-CTT rescues the dorsal body curvature that is produced both by inhibition of PC1 expression and by inhibition of γ-secretase activity in zebrafish. Finally, we provide evidence establishing a common mechanism for PC1-CTT inhibition of proproliferative and proapoptotic signaling pathways through disruption of the relevant transcription factors' interactions with the transcriptional coactivator p300.

RESULTS

Loss of PC1 in Mouse Renal Epithelial Cells Causes Increased Proliferation, Apoptosis, and Cyst Development in 3D Cell Culture

Clonal renal tubular epithelial cell lines derived from *Pkd1*$^{flox/-}$ mice were transfected with Cre recombinase to generate *Pkd1*$^{-/-}$ cells (Joly et al., 2006; Shibazaki et al., 2008). These cell lines, which are genetically identical except for the deletion of both copies of the gene encoding PC1 in the *Pkd1*$^{-/-}$ cells, produced strikingly different multicellular structures when grown in 3D culture. *Pkd1*$^{flox/-}$ cells grew into extended, tubule-like structures, whereas the *Pkd1*$^{-/-}$ cells developed into large, spherical cysts with hollow central lumens (Figure 1A). This can be seen graphically in time-lapse videos of *Pkd1*$^{flox/-}$ and *Pkd1*$^{-/-}$ cells grown in 3D culture (see Movies S1, S2, and S3 available online). The *Pkd1*$^{-/-}$ cells acquire a hollow central lumen within the first several days of culture, whereas the *Pkd1*$^{flox/-}$ cells slowly form linear tubule-like structures.

Pkd1$^{-/-}$ cells displayed higher levels of proliferation as compared to *Pkd1*$^{flox/-}$ cells, as measured by BrdU incorporation (Figure 1B). Apoptosis, as measured by staining for cleaved caspase-3, was virtually undetectable in the *Pkd1*$^{flox/-}$ cells, whereas apoptosis was evident in the *Pkd1*$^{-/-}$ cells, both in cyst-lining cells (Figure 1B, arrowheads) and at the center of cell aggregates that had yet to develop a hollow central lumen (Figure 1B, inset).

To determine the effect of the isolated PC1-CTT on cystogenesis, PC1-CTT was conditionally expressed under the control of doxycycline using a TET-Off inducible expression system in a stably transfected *Pkd1*$^{-/-}$ cell line. *Pkd1*$^{-/-}$ cells induced to express PC1-CTT displayed decreased levels of proliferation, as measured by BrdU incorporation. In addition, expression of PC1-CTT in the *Pkd1*$^{-/-}$ cells resulted in a dramatic change in the morphology of the structures they formed in 3D culture. Instead of large, hollow-lumen, cyst-like structures, the *Pkd1*$^{-/-}$ cells that express the PC1-CTT developed into branched tubule-like structures lacking a hollow central lumen (Figure 1C). The average sizes of the structures formed by the *Pkd1*$^{-/-}$ cells that express the PC1-CTT were similar to those measured for the parental *Pkd1*$^{flox/-}$ cells, and these structures were significantly smaller than the cystic structures formed by the *Pkd1*$^{-/-}$ cells (Figures 1D and 1E). Immunostaining performed with an antibody directed against the HA epitope appended to the PC1-CTT construct demonstrates that these small cell clusters and tubule-like structures do indeed express the exogenous PC1-CTT protein (shown in red in Figure 1C and in gray scale in the lower right panel of Figure 1D) and that the PC1-CTT protein is concentrated in the nucleus (Figure S1).

The CTT Cleavage of PC1 Is Dependent upon γ-Secretase

C-terminal cleavage of PC1 was detected in HEK cells transfected with a cDNA construct encoding full-length PC1 tagged at the C terminus with the DNA-binding domain of Gal4 (Bertuccio et al., 2009). Cleavage of PC1 allows the released CTT-Gal4 to translocate to the nucleus and to stimulate luciferase production from a cotransfected UAS-Luciferase reporter plasmid. Assays are performed in the presence of clasto-lactacystin, to prevent proteasome degradation of the cleaved PC1-CTT (Bertuccio et al., 2009). The γ-secretase inhibitor DAPT was added to the media after transfection, and the cells were incubated for 24 hr (Shearman et al., 2000). PC1 cleavage, as measured by Gal4-driven luciferase expression, was inhibited in a dose-dependent manner by DAPT, indicating that PC1-CTT cleavage is dependent upon γ-secretase activity (Figure 2A).

Further evidence for γ-secretase-dependent cleavage of PC1 was obtained through DAPT treatment of LLC-PK$_1$ cells stably expressing a full-length PC1 construct that carries a C-terminal HA tag. Lysates from cells treated with clasto-lactacystin (to prevent proteasome degradation of cleaved PC1 fragments) were fractionated to separate nuclei from cytoplasm, and the resultant fractions were analyzed by immunoblot. Bands corresponding to the cleaved PC1-CTT were detected predominantly in the nuclear fractions, and the intensity of this complex of bands was significantly decreased in cells exposed to DAPT (Figure 2B). We used siRNA to knock down expression in HEK293 cells of Presenilin-1 or Presenilin-2, each of which can serve as the catalytic subunit of the functional γ-secretase complex. Loss of Presenilin-1 did not decrease PC1-CTT cleavage as measured by the PC1-GalVP cleavage assay (Figure 2C, left panels). Presenilin-2 knockdown, however, resulted in a significant decrease in PC1-CTT cleavage (Figure 2C, right panels) and a reduction in the nuclear accumulation of PC1 cleavage products (Figure S2).

We next wished to determine whether γ-secretase-mediated cleavage of PC1 is required for the PC1 protein to exert its effects on epithelial morphogenesis. *Pkd1*$^{flox/-}$ cells cultured in 3D were treated with either DMSO vehicle or with DAPT for 10 days. DAPT treatment resulted in a significant change in morphology in the *Pkd1*$^{flox/-}$ cells. Whereas DMSO-treated cells formed linear tubule-like structures, DAPT-treated cells formed spherical cyst-like structures with hollow central lumens (Figure 2D, left panels) reminiscent of the structures formed by the *Pkd1*$^{-/-}$ cells. DAPT treatment had no significant effect on the morphology of *Pkd1*$^{-/-}$ cells (Figure 2D, right panels).

Expression of PC1-CTT Results in Reduced Proliferation and Apoptosis in Pkd1$^{-/-}$ Cells

To quantify the effects observed in the 3D cell culture system, *Pkd1*$^{flox/-}$ and *Pkd1*$^{-/-}$ cells were cultured in two dimensions on glass coverslips, and BrdU incorporation (Figure 3A) and cleaved caspase-3 staining (Figure S3) were assessed as measures of proliferation and apoptosis, respectively. *Pkd1*$^{-/-}$ cells displayed a significantly higher level of proliferation than *Pkd1*$^{flox/-}$ controls. However, reintroduction of the isolated PC1-CTT significantly reduced proliferation of the *Pkd1*$^{-/-}$ cells to levels similar to those observed in *Pkd1*$^{flox/-}$ cells (Figure 3B). Similarly, *Pkd1*$^{-/-}$ cells displayed a significantly higher level of apoptosis when compared to *Pkd1*$^{flox/-}$ controls. When PC1-CTT expression was induced in Pkd1$^{-/-}$ cells, the level of apoptosis decreased significantly. Expression of PC1-CTT in the *Pkd1*$^{-/-}$ cells reduced apoptosis to levels similar to those seen in the *Pkd1*$^{flox/-}$ cells (Figure 3C; Figure S3).

PC1-CTT Directly Interacts with TCF and Inhibits Canonical Wnt Signaling

Previous data implicate canonical Wnt signaling as a driver of cyst proliferation. Recent studies show activation of Wnt target

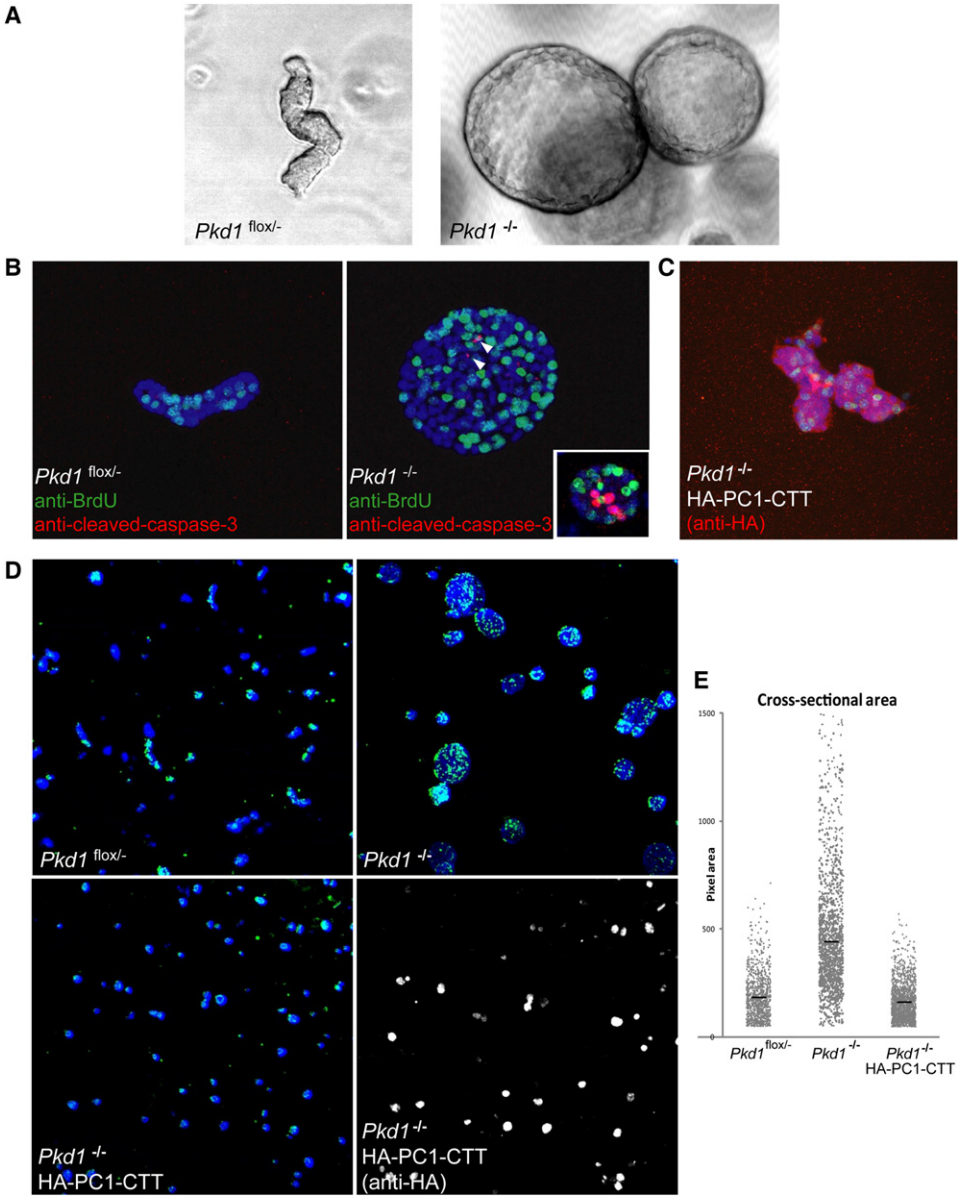

Figure 1. *Pkd1* Knockout Results in Increased Proliferation, Apoptosis, and Cystic Morphology

(A) Phase-contrast imaging of *Pkd1*$^{flox/-}$ and *Pkd1*$^{-/-}$ cells grown in 3D Matrigel matrix for 10 days.

(B) *Pkd1*$^{flox/-}$ and *Pkd1*$^{-/-}$ structures were incubated with BrdU, fixed, and stained with α-BrdU-FITC (green) and α-cleaved caspase-3 (red). Nuclei were counterstained with Hoechst 33342 (blue). The inset depicts a cell aggregate that had yet to develop a hollow central lumen.

(C) *Pkd1*$^{-/-}$ cells stably expressing HA-PC1-CTT were grown in 3D Matrigel matrix for 10 days, exposed to BrdU, fixed, and stained with α-BrdU-FITC (green) and α-HA (red) to detect expression of the HA-PC1-CTT. Nuclei were counterstained with Hoechst 33342 (blue). Cellular structures were imaged on a Leica confocal microscope using a 40× objective.

(D) The top two panels show *Pkd1*$^{flox/-}$ and *Pkd1*$^{-/-}$ cells that were grown in 3D Matrigel matrix for 7 days, incubated with BrdU, and then stained with α-BrdU (green). Nuclei were counterstained with Hoechst 33342 (blue). The bottom two panels show *Pkd1*$^{-/-}$ cells stably expressing HA-PC1-CTT that were grown in 3D Matrigel matrix for 7 days, incubated with BrdU, and then stained with α-BrdU (green). Nuclei were counterstained with Hoechst 33342 (blue, left), and CTT expression was detected with α-HA (gray, right).

(E) Plot of cross-sectional area of cellular structures pictured in (D). Bars indicate mean area in pixels: *Pkd1*$^{flox/-}$ = 185, *Pkd1*$^{-/-}$ = 447, *Pkd1*$^{-/-}$ HA-PC1-CTT = 163, n = 1,000 for each condition.

genes in cells derived from human ADPKD cystic tissue and demonstrate an interaction between the PC1-CTT and components of the Wnt-signaling pathway (Kim et al., 1999; Lal et al., 2008; Zhang et al., 2007). The Wnt pathway regulates the size and activity of the cytosolic pool of β-catenin. At the cell membrane, β-catenin is bound by E-cadherin. In resting polarized epithelial cells, β-catenin is predominantly sequestered at the basolateral plasma membrane, where it participates in the

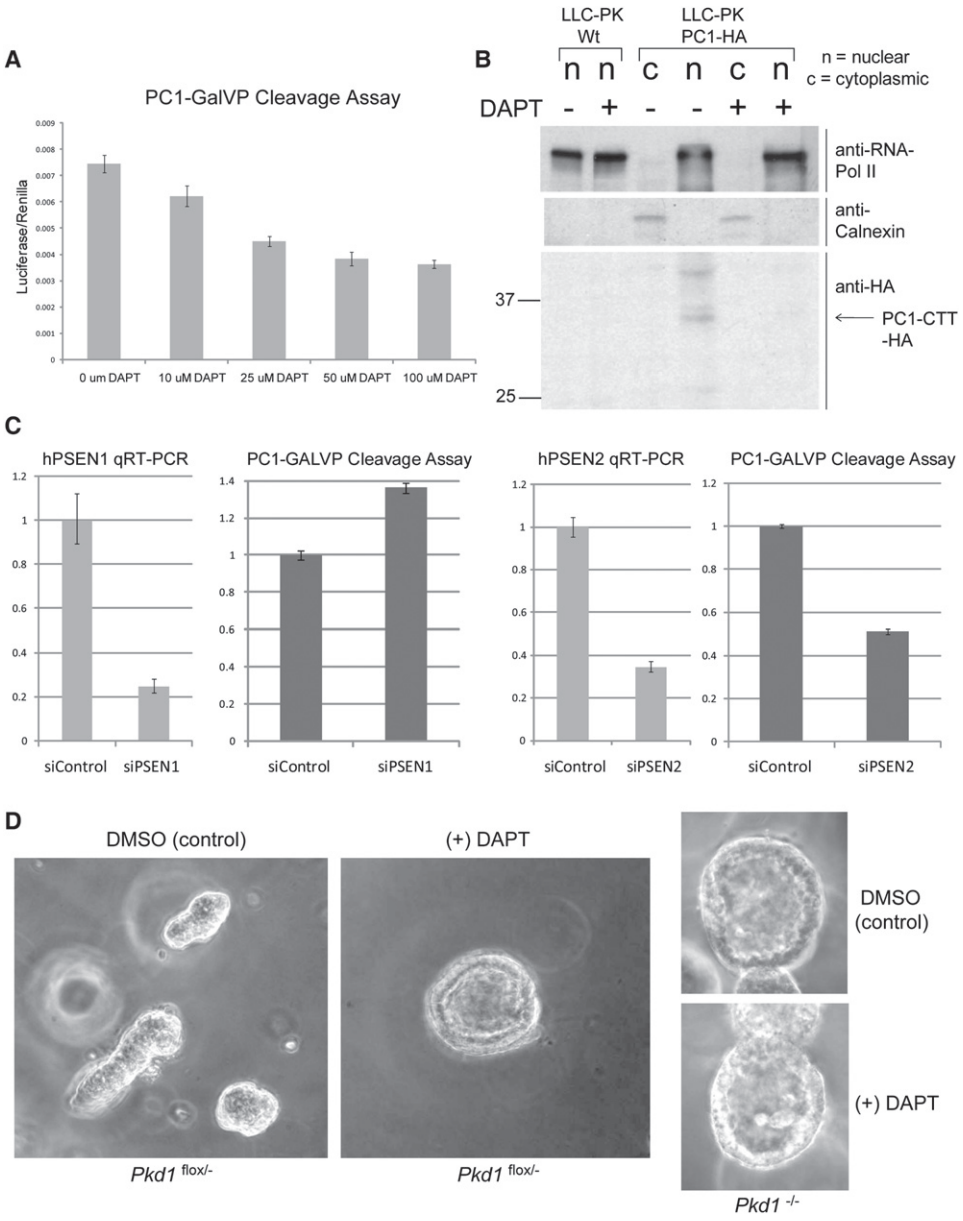

Figure 2. PC1-CTT Cleavage Is Sensitive to the γ-Secretase Inhibitor DAPT

(A) HEK293 cells transfected with PC1-GalVP, UAS-Luciferase, and Renilla were treated with the γ-secretase inhibitor DAPT at the indicated concentrations in the presence of clasto-lactacystin for 24 hr prior to quantification of the luciferase signal.

(B) LLC-PK$_1$ cells stably expressing full-length PC1 with a C-terminal 2× HA tag were exposed to DAPT for 24 hr, in the presence of clasto-lactacystin, before nuclear/cytoplasmic fractionation. Proteins were separated on a 10% SDS-polyacrylamide gel and analyzed by immunoblot. Nuclear purification was assessed using α-RNA-Pol II (nuclear fraction) and α-calnexin (nonnuclear fraction). PC1-CTT cleavage fragments were detected using α-HA.

(C) HEK293 cells were transfected with either siControl (nontargeting RNA) or siRNA directed against human Presenilin-1 or Presenilin-2. qRT-PCR was used to determine knockdown efficiency. PC1-GalVP, UAS-Luciferase, and Renilla were super-transfected into HEK cells after 48 hr of siRNA treatment to report on PC1-CTT cleavage. Data are mean ± SE of four replicates each from two independent experiments. The data in all four panels are normalized to the siControl condition.

(D) *Pkd1*$^{flox/-}$ and *Pkd1*$^{-/-}$ cells were cultured in 3D Matrigel matrix for 10 days in media containing either DMSO (vehicle control) or 100 μM DAPT, after which they were fixed and imaged on a phase-contrast microscope.

formation of E-cadherin-dependent adhesive junctions. Free cytoplasmic β-catenin is recognized by a "destruction complex" that mediates its phosphorylation, targeting it for proteosomal degradation. Activation of Wnt signaling prevents the destruction of free cytosolic β-catenin, which enters the nucleus to serve as a coactivator of the TCF transcription factor and thus induces proliferation (Daugherty and Gottardi, 2007). To measure endogenous Wnt-signaling activity, we employed the TopFlash assay, which utilizes a TCF-binding promoter element to drive expression of a luciferase reporter (van de Wetering et al., 1997).

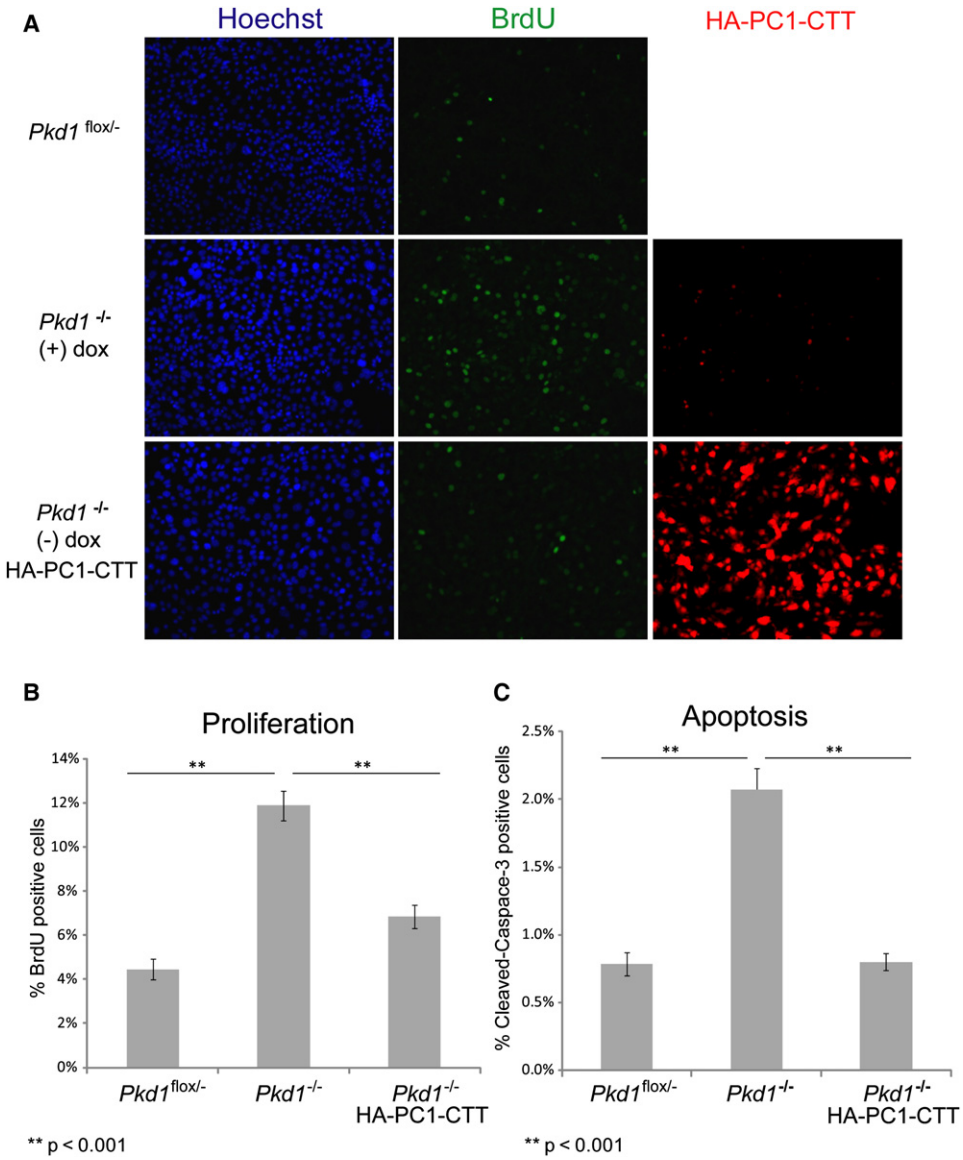

Figure 3. Effects of PC1-CTT Expression on Proliferation and Apoptosis

(A) *Pkd1*$^{flox/-}$ and *Pkd1*$^{-/-}$ cells stably expressing HA-PC1-CTT encoded by a TET-Off inducible vector were grown on coverslips. PC1-CTT expression was induced in the *Pkd1*$^{-/-}$ cell line by withdrawal of doxycycline for 48 hr prior to BrdU exposure and fixation. Proliferating cells were labeled with α-BrdU-FITC (green), PC1-CTT expression was detected with α-HA (red), and nuclei were counterstained with Hoechst 33342 (blue).

(B) Proliferation was quantified using automated cell-counting software. Expression of PC1-CTT in *Pkd1*$^{-/-}$ cells resulted in a reduction of proliferation to levels approaching those observed in the *Pkd1*$^{flox/-}$ cells.

(C) Apoptosis was assessed by staining with an antibody directed against cleaved caspase-3 (Figure S3) and quantified using automated cell-counting software. Expression of PC1-CTT in *Pkd1*$^{-/-}$ cells resulted in a reduction in apoptosis to levels similar to those seen in the *Pkd1*$^{flox/-}$ cells. Data are mean ± SE of ten fields each from three independent experiments.

Pkd1$^{-/-}$ cells demonstrated significantly higher levels of TCF activity than did the *Pkd1*$^{flox/-}$ controls. Furthermore, expression of PC1-CTT in the *Pkd1*$^{-/-}$ cells resulted in a significant reduction in the TopFlash luciferase activity to levels similar to those detected in *Pkd1*$^{flox/-}$ cells (Figure 4A). This activity is dependent upon the presence of the PC1-CTT nuclear localization sequence (NLS), as evidenced by the fact that a PC1-CTT construct lacking the NLS (PC1-CTT-ΔNLS) (Chauvet et al., 2004) does not exert any inhibitory influence on TopFlash activity (Lal et al., 2008; Figure 4B). Although the PC1-CTT-ΔNLS construct does not alter TopFlash activity, it is worth noting that this construct is able to produce a significant signal in a reporter assay that measures the activity of the STAT6 pathway (Figure 4C). These data, which are consistent with previous observations indicating that portions of the PC1-CTT can activate STAT6 signaling (Low et al., 2006), demonstrate that loss of the NLS selectively blocks some but not all of the functional activities of the PC1-CTT.

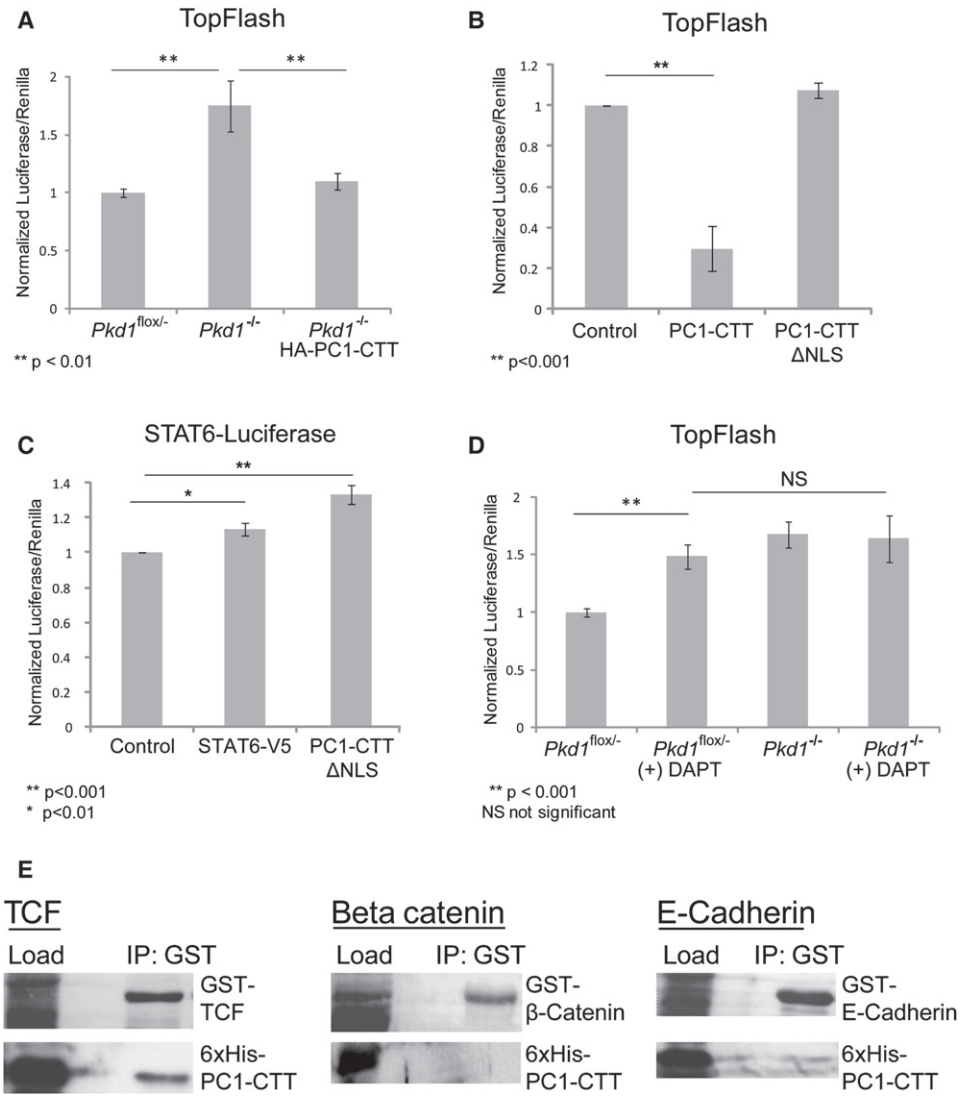

Figure 4. TopFlash Activity Is Elevated in *Pkd1*$^{-/-}$ Cells and Inhibited by PC1-CTT Expression

(A) *Pkd1*$^{flox/-}$ and *Pkd1*$^{-/-}$ cells stably expressing HA-PC1-CTT in a TET-Off inducible vector were transfected with TopFlash and Renilla luciferase reporter constructs in the presence or absence of doxycycline, and luciferase activity was measured 24 hr later.

(B) TopFlash activity is significantly inhibited by expression of the PC1-CTT in HEK293 cells. Expression of the PC1-CTTΔNLS does not inhibit TopFlash activity.

(C) HEK293 cells were transfected with a luciferase reporter construct driven by a STAT6-responsive promoter, as a measure of STAT6 activation. Expression of exogenous STAT6, or PC1-CTTΔNLS results in a significant activation of STAT6 promoter-driven luciferase production.

(D) *Pkd1*$^{flox/-}$ and *Pkd1*$^{-/-}$ cells were transfected with TopFlash and Renilla luciferase reporter constructs and exposed to the γ-secretase inhibitor DAPT for 24 hr prior to quantification of luciferase signal. Data are mean ± SE of four replicates each from three independent experiments.

(E) GST-tagged constructs corresponding to the β-catenin-binding domain of TCF, E-cadherin CTT, and β-catenin were coexpressed with His-tagged PC1-CTT in bacteria. When precipitated with glutathione beads, the PC1-CTT displays a strong direct interaction with TCF, and little direct interaction with E-cadherin or β-catenin.

Treatment of *Pkd1*$^{flox/-}$ cells with DAPT abolished the inhibitory effect of PC1 expression on TopFlash activity, consistent with the hypothesis that PC1-CTT cleavage and nuclear translocation of the released CTT fragment are necessary for its inhibitory effect on TCF. DAPT treatment of *Pkd1*$^{-/-}$ cells did not stimulate any further increase in TopFlash activity, indicating that the increase in Wnt activity obtained through inhibition of γ-secretase is dependent on the presence of PC1 (Figure 4D).

To dissect further the elements of the canonical Wnt-signaling pathway that interact directly with PC1-CTT, a bacterial coexpression system was employed to drive simultaneous expression of a His-tagged PC1-CTT and of GST-tagged polypeptides incorporating the sequences of β-catenin, the E-cadherin cytoplasmic domain, or TCF. When bacterial lysates were subjected to glutathione-Sepharose pull-down and the recovered proteins were blotted with anti-His antibody, PC1-CTT exhibited little direct interaction with β-catenin or with

E-cadherin but showed a strong direct physical interaction with TCF (Figure 4C).

PC1-CTT Interacts with CHOP and Inhibits Its Activity

Data suggesting that the PC1-CTT may regulate apoptosis (Figures 1 and 3; Figure S3) led us to search for novel regulatory targets that could mediate this influence. To identify transcription factors regulated by PC1-CTT, we employed a "coactivator trap" screen, in which over 800 transcription factors are fused to the DNA-binding domain of Gal4 (Amelio et al., 2007). After cotransfection of each transcription factor-Gal4 construct and a Gal4-driven luciferase reporter vector into HEK293 cells, luciferase assays established baseline activities for each transcription factor. PC1-CTT was then cotransfected, and any effect of PC1-CTT on each transcription factor's activity was measured as a change in luciferase production as compared to its baseline level. Several transcription factors were found to be significantly regulated in the presence of PC1-CTT. One of the most profoundly affected was CHOP-10/GADD153, which induces apoptosis in response to ER stress as part of the unfolded protein response (UPR) (Oyadomari and Mori, 2004) (Table S1).

To measure the effects of full-length PC1 expression on CHOP activation, *Pkd1*$^{flox/-}$ and *Pkd1*$^{-/-}$ cells were transfected with the CHOP-Gal4 and the Gal4-luciferase reporter constructs. *Pkd1*$^{-/-}$ cells displayed significantly higher levels of CHOP activity when compared to the *Pkd1*$^{flox/-}$ cells. Expression of the soluble PC1-CTT in the *Pkd1*$^{-/-}$ cells resulted in a significant inhibition of CHOP-Gal4 activity (Figure 5A). In addition, treatment of *Pkd1*$^{flox/-}$ cells with DAPT abolished the inhibitory effect that PC1 expression exerts on CHOP-Gal4 activity. DAPT treatment of *Pkd1*$^{-/-}$ cells did not stimulate a further elevation in CHOP activity, indicating that the increase in CHOP activity obtained through inhibition of γ-secretase-dependent protein cleavage is dependent on the presence of PC1 (Figure 5B). Thus, the presence of the PC1 protein acts, via its released CTT, to negatively regulate CHOP activity. Once again, this activity is dependent upon the presence of the PC1-CTT NLS because the PC1-CTT-ΔNLS construct does not exert any inhibitory influence on CHOP activity (Figure 5C). To determine whether the increased rate of apoptosis observed in the *Pkd1*$^{-/-}$ cells is indeed a consequence of CHOP activity, *Pkd1*$^{-/-}$ and *Pkd1*$^{flox/-}$ cells were subjected to siRNA-mediated knockdown of CHOP expression. Apoptosis was scored by staining for cleaved caspase-3 (Figure 5D). Consistent with the data shown in Figure 3C, the apoptotic rate manifest by the *Pkd1*$^{-/-}$ cells transfected with a control siRNA was twice that observed for the similarly treated *Pkd1*$^{flox/-}$ cells. Whereas knockdown of CHOP expression had no effect on the apoptotic rate observed in the *Pkd1*$^{flox/-}$ cells, treatment with the CHOP siRNA reduced the apoptotic rate in the *Pkd1*$^{-/-}$ cells to the level measured in the *Pkd1*$^{flox/-}$ cells. Taken together, these data demonstrate that PC1 reduces CHOP activity in a cleavage-dependent manner, and that elevated CHOP activity accounts for the increased apoptosis that is measured in cells that lack PC1 expression.

To assess the possibility of a physical interaction between CHOP and the PC1-CTT, HEK cells were transfected with constructs encoding HA-PC1-CTT and a FLAG-tagged CHOP protein. Lysates prepared from these cells were subjected to immunoprecipitation with anti-HA beads. CHOP coprecipitated with the soluble PC1-CTT construct (Figure 5E). This interaction was further validated by immunoprecipitation experiments performed on lysates of nuclear fractions prepared from LLC-PK$_1$ cells stably expressing a full-length PC1 that carries a C-terminal HA tag (Chapin et al., 2010). The endogenously cleaved PC1-CTT released from the full-length PC1 protein coprecipitated with nuclear CHOP (Figure 5F).

PC1-CTT Inhibits TCF and CHOP Activities by Disrupting Their Interactions with p300

Although TCF and CHOP activate discrete transcriptional pathways, they both utilize and depend upon the common transcriptional coactivator, p300/CBP (Li et al., 2007; Ohoka et al., 2007). To determine the potential importance of p300 in the PC1-CTT-mediated regulation of TCF and CHOP, HEK cells were transfected with PC1-CTT alone, or in the presence of overexpressed p300. As shown previously, PC1-CTT expression inhibits TCF activity (as assessed by TopFlash assay) in the context of native levels of p300 protein expression (Lal et al., 2008). Overexpression of p300 eliminated this inhibitory effect of PC1-CTT, suggesting that this inhibitory effect is achieved through competition between the PC1-CTT and p300 for binding to TCF (Figure 6A).

To test this possibility directly, TCF and CHOP were precipitated from HEK cells transfected with p300 and PC1-CTT (Figures 6B and 6D). As expected, in the absence of PC1-CTT, TCF and CHOP each coprecipitates with p300 (Hecht and Stemmler, 2003; Ohoka et al., 2007). These interactions were significantly disrupted in cells that express PC1-CTT, suggesting that the CTT of PC1 exerts its inhibitory effect on the activities of TCF and CHOP by interfering with their interactions with p300 (Figures 6B–6E).

PC1-CTT Rescues Morphant Phenotypes in Pkd1-Knockdown Zebrafish Embryos

Morpholino-induced knockdown of the two zebrafish *Pkd1* genes, *Pkd1a* and *Pkd1b*, produces dorsal body axis curvature, kidney cysts, hydrocephalus, and skeletal abnormalities (Mangos et al., 2010). Of these findings, the dorsal body curvature was considered to be the most reliable marker of Pkd1 knockdown, due to the substantially higher penetrance of this phenotype. Interestingly, treatment of zebrafish embryos with the γ-secretase inhibitor DAPT produces a similar phenotype, characterized by mild and moderate dorsal axis curvature (Arslanova et al., 2010). To determine the capacity of the PC1-CTT to rescue the phenotype associated with impaired *Pkd1* gene expression in vivo, zebrafish embryos were injected with Pkd1a/b morpholinos alone, or with mRNA encoding the PC1-CTT. Knockdown of *Pkd1a/b* results in dorsal axis curvature, whereas concurrent injection of the PC1-CTT significantly decreases the severity of the body curvature at 3 dpf (Figures 7A and 7B). Injection of mRNA encoding the PC1-CTT-ΔNLS construct did not rescue the body curvature phenotype (Figures S4A and S4B). A subset of the signaling pathways influenced by the PC1-CTT requires the NLS (Wnt and CHOP), whereas others appear to not require the presence of this motif (e.g., STAT-6) (Figures 4B, 4C, and 5C). Thus, these data suggest that the capacity of the PC1-CTT to ameliorate the severity of the body curvature phenotype involves one or more of the NLS-dependent

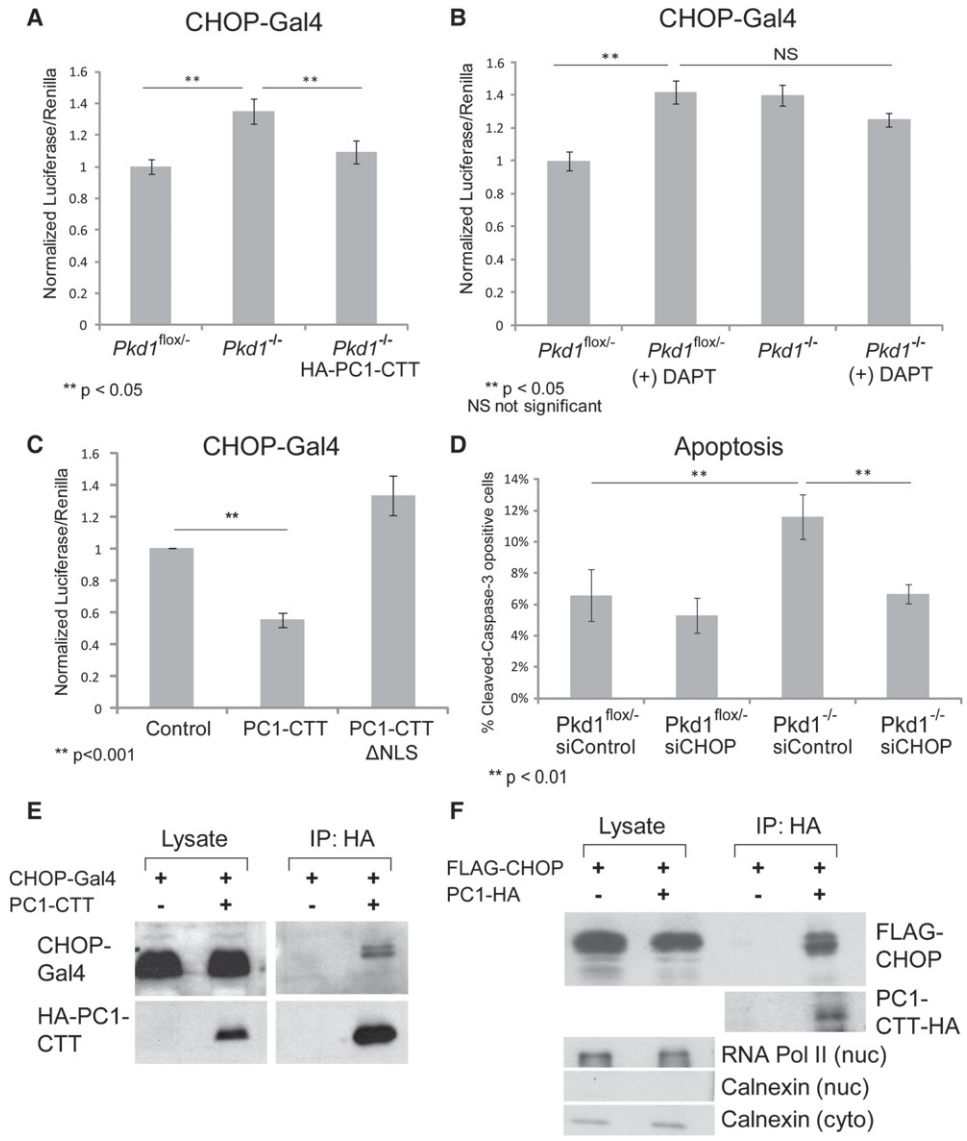

Figure 5. CHOP-Gal4 Activity Is Elevated in Pkd1$^{-/-}$ Cells and Inhibited by PC1-CTT Expression

(A) *Pkd1*$^{flox/-}$ and *Pkd1*$^{-/-}$ cells stably expressing HA-PC1-CTT in a TET-Off inducible vector were transfected with CHOP-Gal4, UAS-Luciferase, and Renilla luciferase reporter constructs in the presence or absence of doxycycline, and luciferase activity was measured 24 hr later.

(B) *Pkd1*$^{flox/-}$ and *Pkd1*$^{-/-}$ cells were transfected with CHOP-Gal4, UAS-Luciferase, and Renilla luciferase reporter constructs and exposed to the γ-secretase inhibitor DAPT for 24 hr prior to quantification of luciferase signal. Data are mean ± SE of four replicates each from three independent experiments.

(C) CHOP-Gal4 activity is significantly inhibited by expression of the PC1-CTT in HEK293 cells, whereas it is not inhibited in the presence of the PC1-CTTΔNLS.

(D) *Pkd1*$^{flox/-}$ and *Pkd1*$^{-/-}$ cells were reverse transfected with either noncoding siRNA (siControl), or siRNA corresponding to CHOP (siCHOP), and apoptosis levels were measured 48 hr later by cleaved caspase-3 staining.

(E) HEK293 cells were cotransfected with CHOP-Gal4 and HA-PC1-CTT. Cell lysates were subjected to immunoprecipitation using α-HA Sepharose, and the immunoprecipitates were then blotted with the indicated antibodies.

(F) LLC-PK$_1$ cells stably expressing full-length PC1 with a C-terminal 2× HA tag were transfected with FLAG-CHOP, and subjected to nuclear/cytoplasmic fractionation. Endogenously cleaved PC1-CTT was immunoprecipitated from the nuclear fraction using α-HA Sepharose, and the resulting complexes were separated on a 10% polyacrylamide gel and blotted with the indicated antibodies.

signaling pathways that are modulated by the PC1-CTT. Finally, injection of mRNA encoding the PC1-CTT, but not mRNA encoding control GFP, partially rescued the body curvature phenotype induced by DAPT treatment, producing a significant increase in the percentage of fish with straight bodies and a decrease in the percentage of moderately curved fish (Figure 7C).

DISCUSSION

Our data confirm the role of PC1 as an inhibitor of renal epithelial cell proliferation and apoptosis, and provide evidence for the mechanism responsible for this regulation, mediated by cleavage and nuclear translocation of the PC1-CTT.

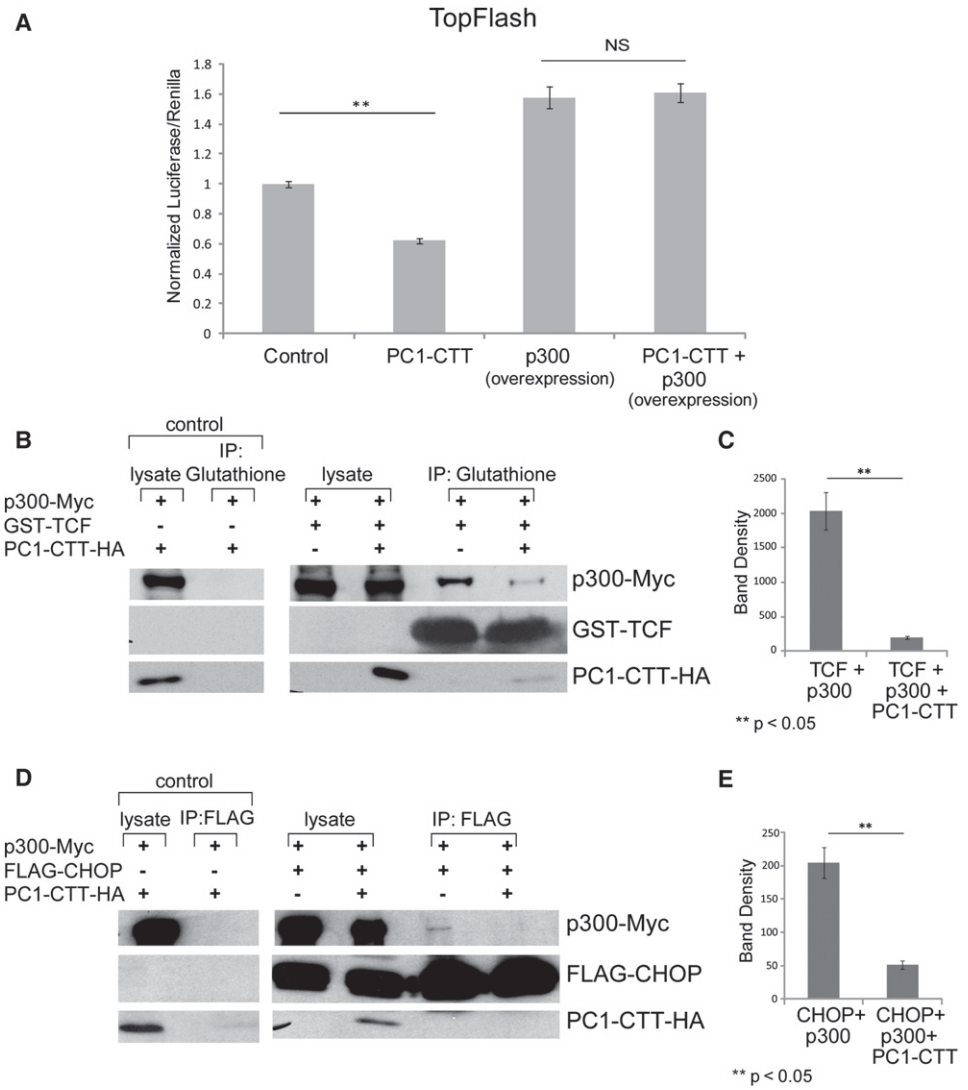

Figure 6. PC1-CTT Competitively Disrupts the Interaction of TCF and CHOP with p300

(A) HEK293 cells were transfected with TopFlash and Renilla luciferase reporter constructs, along with PC1-CTT alone or with PC1-CTT and a construct driving overexpression of full-length p300. NS, not significant.

(B) HEK293 cells were transfected with Myc-p300, and with HA-PC1-CTT where indicated. Cell lysates were incubated with glutathione beads prebound with GST-TCF. Recovered complexes were eluted in SDS-PAGE loading buffer, run on a 10% SDS-polyacrylamide gel, and blotted with the indicated antibodies.

(C and E) Band densitometry was performed using image analysis software to quantitate the data from the coprecipitation experiments shown in (B) and (D). Results are expressed as mean ± SE from four independent experiments.

(D) HEK293 cells were transfected with Myc-p300, FLAG-CHOP, and with HA-PC1-CTT where indicated. Cell lysates were incubated with α-FLAG prebound to agarose beads to precipitate CHOP, and the recovered complexes were eluted in SDS-PAGE loading buffer, run on a 10% SDS- polyacrylamide gel, and blotted with the indicated antibodies.

Reintroduction of the PC1-CTT into *Pkd1* knockout cells is sufficient to normalize their excessive proliferative and apoptotic activities, and the PC1-CTT is sufficient to rescue the dorsal tail curvature phenotype produced by morpholino-mediated disruption of *Pkd1a/b* expression in zebrafish. We show that PC1 cleavage is dependent upon γ-secretase activity, and that the released PC1-CTT inhibits TCF and CHOP, thereby regulating proliferation and apoptosis, respectively. Furthermore, injection of mRNA encoding the PC1-CTT is capable of partially rescuing the dorsal tail curvature phenotype produced by exposure of zebrafish embryos to the γ-secretase inhibitor DAPT. The similarity of the phenotypes produced by *Pkd1a/b* disruption and DAPT treatment is intriguing, and the ability of the PC1-CTT to partially rescue both suggests that at least some of the critical biological activities of the PC1 protein are dependent upon its γ-secretase-dependent PC1-CTT cleavage. Finally, we demonstrate that PC1-CTT inhibits TCF and CHOP by disrupting their interaction with the transcriptional coactivator p300, illustrating a common mechanism through which PC1-CTT is capable of regulating two distinct transcriptional pathways.

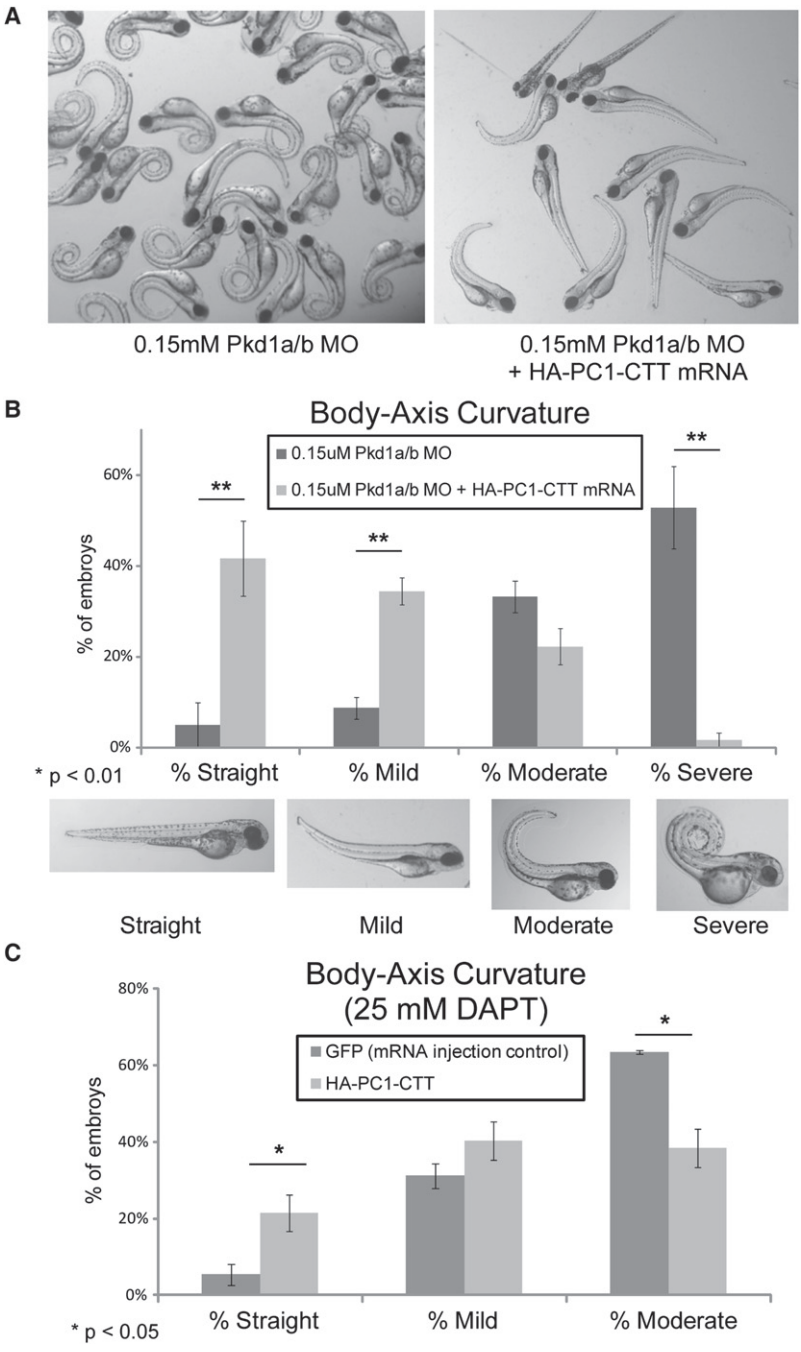

Figure 7. Both Morpholino Knockdown of *Pkd1a/b* and Treatment with DAPT Result in Dorsal Axis Curvature in Zebrafish Embryos, which Can Be Rescued by Expression of the PC1-CTT

(A) Morpholinos corresponding to the zebrafish *Pkd1a* and *Pkd1b* PC1 genes were injected into zebrafish embryos at the one- to two-cell stage to impair expression of the two *Pkd1* genes. The embryos were subsequently injected with 300 nM of mRNA encoding HA-PC1-CTT, where indicated, and imaged at 3 days post fertilization (dpf).

(B) Embryo phenotypes were scored based on the degree of dorsal tail curvature: mild (<90°), moderate (>90°), and severe (tail tip crossing the body axis). The data represent the averages of three separate experiments; error bars represent SEM.

(C) Embryos were injected with 300 nM mRNA encoding either GFP (control) or HA-PC1-CTT at the one- to two-cell stage, then immersed in embryo media containing 25 μM DAPT, imaged at 3 dpf, and scored for the tail curvature phenotype.

Hyperproliferation and increased apoptosis are characteristic of ADPKD (Lanoix et al., 1996; Starremans et al., 2008). We found that loss of *Pkd1* in otherwise genetically identical cell lines resulted in a significant increase in both proliferation and apoptosis. These experiments were performed in vitro, thus eliminating any potential effects of the cyst microenvironment on the proliferative or apoptotic potential of the cyst-lining cells that might complicate the situation in vivo. Thus, our data establish that the loss of expression of the *Pkd1* gene product is primarily responsible for the proliferative and apoptotic changes seen in ADPKD.

Cleavage of the CTT of PC1 has been observed in several studies (Bertuccio et al., 2009; Chauvet et al., 2004; Lal et al., 2008; Low et al., 2006), and its subsequent translocation to the nucleus strongly implies its role in the regulation of transcriptional pathways. Although the cleaved CTT fragment certainly does not recapitulate all of the functions of full-length PC1, our data suggest that the isolated CTT is sufficient to reestablish normal low levels of proliferation and apoptosis, and of TCF and CHOP activity, when expressed in *Pkd1* knockout cells. Furthermore, PC1-CTT is capable of at least partially restoring to *Pkd1* knockout cells the tubular morphology that is obtained with wild-type and *Pkd1* heterozygous cells grown in 3D cell culture. Finally, our data suggest that PC1 cleavage by γ-secretase may be necessary for PC1 to mediate its full complement of physiological functions. Inhibiting γ-secretase activity causes PC1-expressing cells that form tubular structures in 3D culture to recapitulate the cystic morphology normally manifest by *Pkd1* null cells. It is possible, of course, that γ-secretase influences epithelial morphogenesis in this assay via additional pathways that are independent of PC1. Because *Pkd1*$^{-/-}$ cells were unaffected by DAPT treatment in both the morphogenesis and the TCF and CHOP assays, however, we conclude that γ-secretase-mediated cleavage of PC1 plays an obligate role in at least a subset of this protein's physiological functions.

The shedding of the extracellular domain of PC1 and the cleavage and nuclear translocation of its cytoplasmic domain together mark PC1 as a member of a growing collection of plasma membrane proteins that is cleaved by γ-secretase and participates in direct signaling to the nucleus (Lal and Caplan, 2011). This behavior is exemplified by the Notch (Fortini, 2009),

EpCAM (Maetzel et al., 2009), and DCC pathways (Taniguchi et al., 2003). The precise site at which γ-secretase cleaves PC1-CTT has not yet been determined. It is worth noting, however, that γ-secretase appears to exhibit substantial promiscuity in the sequence compositions of its substrate cleavage sites (Beel and Sanders, 2008; Struhl and Adachi, 2000). This promiscuity may account, at least in part, for the number of discrete PC1-CTT cleavage products that can be detected in nuclear fractions (Figure 2B). The precise signals that stimulate γ-secretase-mediated cleavage of PC1 have yet to be discovered.

We report a direct physical interaction between the PC1-CTT and TCF. Lal et al. have suggested that the PC1-CTT inhibits canonical Wnt signaling through an interaction with β-catenin (Lal et al., 2008). Because these experiments assessed the coimmunoprecipitation of epitope-tagged proteins coexpressed in human cell lines, the recovered protein complexes may have contained additional members of the signaling pathway, such as TCF, that were not detected in immunoblots that assessed only the presence of the tagged proteins. Thus, it seems likely that the coprecipitation of the PC1-CCT and β-catenin observed by Lal et al. (Lal et al., 2008) could be attributable to a mutual interaction of both of these proteins with TCF to form an inactive tertiary complex. The bacterial coexpression system utilized in the present study allowed us to further dissect the canonical Wnt pathway and to determine that TCF is a direct binding partner of PC1-CTT. It should be noted that, while activation of the Wnt-signaling pathway is sufficient to produce renal cystic disease (Qian et al., 2005; Saadi-Kheddouci et al., 2001), and markers of Wnt signaling appear to be elevated in the context of human ADPKD (Lal et al., 2008), a recent study found that the cyst-lining cells of mouse models of ADPKD that express a Wnt/TCF reporter did not manifest elevated levels of Wnt activity (Miller et al., 2011). Therefore, it is possible that activation of Tcf-mediated transcription plays an early, transient role in the initiation of cyst formation that is terminated by the time cysts are manifest. It is also possible that pathways other than those associated with Wnt/TCF drive the hyperproliferation that is associated with the cystic epithelial cells in ADPKD. In either case, our data demonstrate that cleavage of the PC1 generates a protein that is both antiproliferative and sufficient to suppress ADPKD-related phenotypes in vitro and in vivo.

The activities of both TCF and CHOP depend upon the common transcriptional coactivator p300 (Li et al., 2007; Ohoka et al., 2007). Our data suggest that PC1-CTT binds directly to the transcription factors TCF and CHOP, and are consistent with the hypothesis that PC1-CTT acts by blocking the p300 binding sites on both TCF and CHOP. Therefore, the p300 protein constitutes a promising convergence point that appears to be utilized by PC1-CTT to regulate two distinct transcription factors. This regulation of TCF and CHOP through interactions with the released PC1-CTT provides a simple and compelling explanation for the dysregulation of proliferation and apoptosis seen in ADPKD.

EXPERIMENTAL PROCEDURES

Antibodies, Plasmids, and Cell Lines

The following antibodies and labeling reagents were used: α-HA antibody, Rat (Roche), FITC α-BrdU Kit (BD Bioscience), α-cleaved caspase-3 (Cell Signaling Technology), α-RNA Pol II (Santa Cruz Biotechnology), α-calnexin (Stratagene), α-His (QIAGEN), α-GST (Amersham), and α-FLAG and α-cMyc (Sigma-Aldrich). For laser-scanning fluorescence microscopy, dye-coupled Alexa antibodies (Alexa 488, 594; Molecular Probes) were used as secondary reagents.

The sequence encoding the final 200 amino acids of human PC1 (4102–4302), containing a 2× HA tag at the N terminus, was cloned into the pNRTis-21 vector (Tenev et al., 2000). The sequence for human PC1-CTT (residues 4102–4302 of Pkd1) was modified by deleting residues 4134–4154, corresponding to the putative NLS to generate the PC1-CTTΔNLS (Chauvet et al., 2004). Stable cell lines were generated by transfection using Lipofectamine 2000 (Invitrogen) and selection with 350 μg ml^{-1} Zeocin (Invitrogen). Expression was inhibited with 100 ng ml^{-1} doxycycline. Full-length human PC1 was cloned into pcDNA3.1.neo (Invitrogen) with 2× HA tag or Gal4VP16 appended to the C terminus as described (Bertuccio et al., 2009). Stable cell clones were selected with 2 mg ml^{-1} Geneticin (GIBCO). GL4.31[luc2P/GAL4UAS] (Promega, Madison, WI, USA) was used as a Gal4 promoter-driven firefly luciferase reporter construct. The TopFlash plasmid was purchased from Upstate Biotechnology. pRL-TK, a vector constitutively expressing Renilla luciferase, was included as an internal control to normalize for transfection differences. The sequence encoding the PC1-CTT was cloned into the pETDuet vector with an N-terminal 6xHis tag, along with either the GST-E-cadherin cytoplasmic domain, GST-β-catenin, or GST-TCF β-catenin binding region (Gottardi and Gumbiner, 2004). The CHOP-Gal4 construct was provided by Dr. John Hogenesch (Department of Pharmacology, University of Pennsylvania). The sequence encoding full-length CHOP was cloned into the pCMV-3Tag-1A vector (Stratagene) to generate 3xFLAG-CHOP. The sequence encoding human p300 (full-length or amino acid residues 1–664) was cloned into the pCMV-Tag 3B vector (Stratagene) to generate Myc-p300.

HEK293T cells (Chauvet et al., 2004), LLC-PK_1 cells, and *Pkd1*$^{flox/-}$ and *Pkd1*$^{-/-}$ temperature-sensitive SV40 large T antigen renal proximal tubule cells (Joly et al., 2006; Shibazaki et al., 2008) were maintained as described.

3D Cell Culture, α-BrdU Staining, and Cell Counting

Pkd1$^{flox/-}$, *Pkd1*$^{-/-}$, and *Pkd1*$^{-/-}$ stably expressing pNRTis HA-PC1-CTT were trypsinized and mixed with 300 μl liquid Matrigel (BD Biosciences) and allowed to solidify for 30 min at 37°C, after which media were added with or without 100 ng ml^{-1} doxycycline, and the cells were grown for 7–10 days. These cell lines were grown on coverslips in parallel for quantification of proliferation and apoptosis.

BrdU was added to the media for 90 min prior to fixation. Cells grown on coverslips were stained as per BD protocol. Cells grown in Matrigel were fixed for 1.5 hr at 37°C, permeabilized for 30 min at 4°C, refixed for 15 min at RT, treated with DNase for 3 hr at 37°C, incubated with the α-BrdU 1°Ab (1:100) for 5 days at 4°C, followed by three 2 hr washes, and by incubation for 1 day with 2°Ab (1:200); nuclei were stained with Hoechst 33342 (Molecular Probes).

Cells grown on coverslips were imaged using an Olympus BX51 epifluorescent microscope equipped with a 20× objective. The percentages of BrdU or caspase-3-positive cells were quantified using a threshold method in conjunction with the ImageJ software package plug-in "Nucleus Counter."

The cross-sectional areas of the cell structures grown in 3D Matrigel culture were calculated using ImageJ software. Cells were stained with α-BrdU, α-HA, and Hoechst 33342 and imaged using an Olympus BX51 epifluorescent microscope equipped with a 10× objective. Cell structures were thresholded from background, and the cross-sectional area of each cell cluster was calculated using the ImageJ Analyze Particles plug-in, with a minimum size cutoff of 50 pixels to filter out isolated cells and debris.

Cell Fractionation

Preparation of nuclear and cytoplasmic fractions was performed as previously described (Chauvet et al., 2004). Cells grown in 10 cm dishes in the presence of 25 μM clasto-lactacystin were harvested in cold PBS, centrifuged for 5 min at 500 × *g*, and resuspended in hypotonic buffer (10 mM HEPES, 1.5 mM MgCl2, 10 mM KCl, and protease inhibitors). Cells were homogenized in a tight-fitting Dounce homogenizer, chilled on ice for 10 min, and then rotated for 15 min. Nonidet P-40 was added to a final concentration of 1%,

and the preparations were rotated for an additional 15 min. The lysates were centrifuged at 1,500 × *g* for 5 min. The resulting supernatant formed the nonnuclear fractions. The pellets (nuclear fractions) were washed in hypotonic buffer for 10 min, resuspended in lysis buffer (50 mM HEPES [pH 7.4], 200 mM NaCl, 0.5% NP-40, 1 mM EDTA, and protease inhibitors), and rotated for 10 min. Pelleted nuclei were lysed by sonication in lysis buffer and prepared for immunoblot analysis. The protein concentration of each sample was determined using a Bio-Rad colorimetric protein concentration assay.

Coactivator Trap Screen

The coactivator trap screen was performed as previously described (Amelio et al., 2007). A pcDNA3.1 construct expressing HA-PC1-CTT was cotransfected with each of 837 transcription factor-Gal4 fusion proteins and the GAL4 luciferase and Renilla reporter plasmids into HEK293Tcells in a 384-well plate. Cells were cultured for 24 hr in a humidified incubator at 37°C in 5% CO_2. Bright-Glo (Promega) reagent (35 μl) was added to each well, and luciferase luminescence was measured with an Acquest plate reader (LJL Biosystems).

Transient Transfection and Luciferase Assay

Pkd1$^{flox/-}$ cells, *Pkd1*$^{-/-}$ cells, and *Pkd1*$^{-/-}$ cells stably expressing pNRTis HA-PC1-CTT were plated in 24-well tissue culture plates and transfected using Lipofectamine 2000 (Invitrogen) at 80%–100% confluency. Luciferase reporter constructs TopFlash or GL4.31[luc2P/GAL4UAS] (0.2 μg), and CHOP-Gal4 (0.05 μg) and pRL-TK (Renilla), were mixed with 2 μl Lipofectamine. HEK293 cells were transfected with STAT6-Luciferase (kind gift of Dr. S.J. Hacque, Cleveland Clinic Foundation) (Haque et al., 1997) or with TopFlash-luciferase, or with CHOP-Gal4/Gal4-luciferase (0.2 μg), as well as with either control plasmid, STAT6-V5, HA-PC1-CTT or HA-PC1-CTTΔNLS, and with pRL-TK (Renilla). Transfection mixtures were added drop wise to cell culture media (containing 80 μM DAPT [Sigma-Aldrich] when indicated) and incubated at 37°C for 24 hr. The amount of DNA in each well was equalized through the addition of a control plasmid, pcDNA3.1, which was also used for mock transfection. Transfected cells were harvested with PBS and lysed with 100 ml of passive lysis buffer (Promega). Luciferase levels were assayed using the Dual Luciferase Assay Reagent kit (Promega). Luciferase signals were determined in a GloMax 20/20 luminometer (Promega).

siRNA Treatment

HEK293 cells were transfected with 100 nM target-specific siRNA or control siRNA using Lipofectamine 2000. As a control siRNA, we used Silencer Negative Control siRNA#1 (#AM4611; Ambion). To knock down PSEN1 and PSEN2, we used validated siRNAs (for PSEN1, SI02662688 from QIAGEN; for PSEN2, AM51331 from Ambion). Knockdown of CHOP was accomplished according a published protocol (Ishikawa et al., 2009).

Immunoprecipitation, Immunoblot, and GST Pull-Down

Cells were lysed by sonication in 50 mM HEPES (pH 7.4), 150 mM NaCl, 0.5% NP-40, 1 mM EDTA with protease inhibitors (Roche). Precleared lysates (18,000 × *g*, 30 min) were incubated at 4°C overnight with either monoclonal-anti-HA agarose, anti-FLAG-M2 agarose (Sigma-Aldrich), or glutathione-Sepharose 4B beads (Amersham) prebound with indicated GST fusion protein constructs harvested from BL21 bacteria by standard procedures (Stratagene). Beads were collected by centrifugation, and the pellets were washed in lysis buffer three times for 10 min with rotation at 4°C. Immunoprecipitates were eluted in SDS-PAGE loading buffer (25 mM Tris-HCl [pH 6.7], 10% glycerol, 1% SDS, 50 mM DTT, bromophenol blue).

Proteins were separated on a 10% SDS-polyacrylamide gel and then electrophoretically transferred to a nitrocellulose membrane (Bio-Rad), incubated in blocking buffer (150 mM NaCl, 20 mM Tris, 5% [w/v] powdered milk, 0.1% Tween) for 60 min, and then incubated with one of the following primary antibodies at 4°C overnight: monoclonal α-HA (rat) antibody (1:5,000; Roche); polyclonal α-FLAG (1:5,000; Sigma-Aldrich); polyclonal α-cMyc (1:5,000; Sigma-Aldrich); polyclonal α-GST (goat) (1:10,000; Amersham); and α-His (1:5,000; QIAGEN). Subsequently, primary antibody binding was detected with horseradish peroxidase-conjugated anti-rat, anti-rabbit, or anti-goat secondary antibodies (1:5,000–10:000; Jackson Labs), and proteins were visualized with an enhanced chemiluminescence detection kit (ECL; Amersham Biosciences).

Zebrafish Experiments: Morpholino Antisense Oligonucleotide and mRNA Injections and Drug Treatment

Morpholino-induced knockdown of *Pkd1a* and *Pkd1b* expression was performed as previously reported (Mangos et al., 2010). Wild-type embryos at the one- to two-cell stage were microinjected with 4.6 nl of a 0.15 mM antisense morpholino oligonucleotide solution (Gene Tools LLC) with 0.1% phenol red using a nanoject2000 microinjector (World Precision Instruments). The sequences of the morpholinos targeting *Pkd1a* and *Pkd1b* were identical to those that have been previously described (Mangos et al., 2010); briefly, the splice donor-blocking oligonucleotide sequences were: *Pkd1a* MO ex8, 5′-GATCTGAGGACTCACTGTGTGATTT-3′; and *Pkd1b* MO ex45, 5′-ACATGA TATTTGTACCTCTTTGGTT-3′. Gene Tools standard negative control morpholino was used as an injection control and demonstrated no effect on development. For drug treatment, after mRNA injection at the one- to two-cell stage, embryos were placed in a 10 cm dish with 30 ml embryo media containing 25 μM DAPT dissolved in DMSO and imaged 3 dpf as described (Arslanova et al., 2010).

Statistical Analysis

Results are expressed as means ± SE. Differences between means were evaluated using Student's t test or analysis of variance as appropriate. Values of $p < 0.05$ were considered to be significant.

SUPPLEMENTAL INFORMATION

Supplemental Information includes four figures, one table, and three movies and can be found with this article online at doi:10.1016/j.devcel.2011.10.028.

ACKNOWLEDGMENTS

We would like to thank Vanathy Rajendran for the generation of PC1 stable cell lines, Arthit Chairoungdua for assistance with live-cell imaging, Lu Zhou for expertise and assistance with zebrafish embryo microinjection, and members of the Caplan laboratory for discussion and advice. We thank Drs. Saikh Jaharul Haque for the gift of the STAT6 reporter reagents and Lloyd Cantley for insightful suggestions. This work was supported by NIH grants HL097800 and NS054794 (J.B.H.), F30DK083227 (D.M.), and DK 57328 and DK090744 (M.J.C., Z.S., and S.S.), by CDMRP PR093488 from the Department of Defense (M.J.C.), and by the Penn Genome Frontiers Institute.

Received: August 25, 2010
Revised: August 1, 2011
Accepted: October 26, 2011
Published online: January 17, 2012

REFERENCES

Amelio, A.L., Miraglia, L.J., Conkright, J.J., Mercer, B.A., Batalov, S., Cavett, V., Orth, A.P., Busby, J., Hogenesch, J.B., and Conkright, M.D. (2007). A coactivator trap identifies NONO (p54nrb) as a component of the cAMP-signaling pathway. Proc. Natl. Acad. Sci. USA *104*, 20314–20319.

Arnould, T., Kim, E., Tsiokas, L., Jochimsen, F., Grüning, W., Chang, J.D., and Walz, G. (1998). The polycystic kidney disease 1 gene product mediates protein kinase C alpha-dependent and c-Jun N-terminal kinase-dependent activation of the transcription factor AP-1. J. Biol. Chem. *273*, 6013–6018.

Arslanova, D., Yang, T., Xu, X., Wong, S.T., Augelli-Szafran, C.E., and Xia, W. (2010). Phenotypic analysis of images of zebrafish treated with Alzheimer's gamma-secretase inhibitors. BMC Biotechnol. *10*, 24.

Beel, A.J., and Sanders, C.R. (2008). Substrate specificity of gamma-secretase and other intramembrane proteases. Cell. Mol. Life Sci. *65*, 1311–1334.

Bertuccio, C.A., Chapin, H.C., Cai, Y., Mistry, K., Chauvet, V., Somlo, S., and Caplan, M.J. (2009). Polycystin-1 C-terminal cleavage is modulated by polycystin-2 expression. J. Biol. Chem. *284*, 21011–21026.

Bhunia, A.K., Piontek, K., Boletta, A., Liu, L., Qian, F., Xu, P.N., Germino, F.J., and Germino, G.G. (2002). PKD1 induces p21(waf1) and regulation of the cell

cycle via direct activation of the JAK-STAT signaling pathway in a process requiring PKD2. Cell *109*, 157–168.

Chapin, H.C., and Caplan, M.J. (2010). The cell biology of polycystic kidney disease. J. Cell Biol. *191*, 701–710.

Chapin, H.C., Rajendran, V., and Caplan, M.J. (2010). Polycystin-1 surface localization is stimulated by polycystin-2 and cleavage at the G protein-coupled receptor proteolytic site. Mol. Biol. Cell *21*, 4338–4348.

Chauvet, V., Tian, X., Husson, H., Grimm, D.H., Wang, T., Hiesberger, T., Igarashi, P., Bennett, A.M., Ibraghimov-Beskrovnaya, O., Somlo, S., and Caplan, M.J. (2004). Mechanical stimuli induce cleavage and nuclear translocation of the polycystin-1 C terminus. J. Clin. Invest. *114*, 1433–1443.

Daugherty, R.L., and Gottardi, C.J. (2007). Phospho-regulation of Beta-catenin adhesion and signaling functions. Physiology (Bethesda) *22*, 303–309.

Fortini, M.E. (2009). Notch signaling: the core pathway and its posttranslational regulation. Dev. Cell *16*, 633–647.

Gottardi, C.J., and Gumbiner, B.M. (2004). Distinct molecular forms of beta-catenin are targeted to adhesive or transcriptional complexes. J. Cell Biol. *167*, 339–349.

Haque, S.J., Wu, Q., Kammer, W., Friedrich, K., Smith, J.M., Kerr, I.M., Stark, G.R., and Williams, B.R. (1997). Receptor-associated constitutive protein tyrosine phosphatase activity controls the kinase function of JAK1. Proc. Natl. Acad. Sci. USA *94*, 8563–8568.

Harris, P.C., and Torres, V.E. (2009). Polycystic kidney disease. Annu. Rev. Med. *60*, 321–337.

Hecht, A., and Stemmler, M.P. (2003). Identification of a promoter-specific transcriptional activation domain at the C terminus of the Wnt effector protein T-cell factor 4. J. Biol. Chem. *278*, 3776–3785.

Hughes, J., Ward, C.J., Peral, B., Aspinwall, R., Clark, K., San Millán, J.L., Gamble, V., and Harris, P.C. (1995). The polycystic kidney disease 1 (PKD1) gene encodes a novel protein with multiple cell recognition domains. Nat. Genet. *10*, 151–160.

Ishikawa, F., Akimoto, T., Yamamoto, H., Araki, Y., Yoshie, T., Mori, K., Hayashi, H., Nose, K., and Shibanuma, M. (2009). Gene expression profiling identifies a role for CHOP during inhibition of the mitochondrial respiratory chain. J. Biochem. *146*, 123–132.

Joly, D., Ishibe, S., Nickel, C., Yu, Z., Somlo, S., and Cantley, L.G. (2006). The polycystin 1-C-terminal fragment stimulates ERK-dependent spreading of renal epithelial cells. J. Biol. Chem. *281*, 26329–26339.

Kim, E., Arnould, T., Sellin, L.K., Benzing, T., Fan, M.J., Grüning, W., Sokol, S.Y., Drummond, I., and Walz, G. (1999). The polycystic kidney disease 1 gene product modulates Wnt signaling. J. Biol. Chem. *274*, 4947–4953.

Lal, M., and Caplan, M. (2011). Regulated intramembrane proteolysis: signaling pathways and biological functions. Physiology (Bethesda) *26*, 34–44.

Lal, M., Song, X., Pluznick, J.L., Di Giovanni, V., Merrick, D.M., Rosenblum, N.D., Chauvet, V., Gottardi, C.J., Pei, Y., and Caplan, M.J. (2008). Polycystin-1 C-terminal tail associates with beta-catenin and inhibits canonical Wnt signaling. Hum. Mol. Genet. *17*, 3105–3117.

Lanoix, J., D'Agati, V., Szabolcs, M., and Trudel, M. (1996). Dysregulation of cellular proliferation and apoptosis mediates human autosomal dominant polycystic kidney disease (ADPKD). Oncogene *13*, 1153–1160.

Li, J., Sutter, C., Parker, D.S., Blauwkamp, T., Fang, M., and Cadigan, K.M. (2007). CBP/p300 are bimodal regulators of Wnt signaling. EMBO J. *26*, 2284–2294.

Low, S.H., Vasanth, S., Larson, C.H., Mukherjee, S., Sharma, N., Kinter, M.T., Kane, M.E., Obara, T., and Weimbs, T. (2006). Polycystin-1, STAT6, and P100 function in a pathway that transduces ciliary mechanosensation and is activated in polycystic kidney disease. Dev. Cell *10*, 57–69.

Maetzel, D., Denzel, S., Mack, B., Canis, M., Went, P., Benk, M., Kieu, C., Papior, P., Baeuerle, P.A., Munz, M., and Gires, O. (2009). Nuclear signalling by tumour-associated antigen EpCAM. Nat. Cell Biol. *11*, 162–171.

Mangos, S., Lam, P.Y., Zhao, A., Liu, Y., Mudumana, S., Vasilyev, A., Liu, A., and Drummond, I.A. (2010). The ADPKD genes pkd1a/b and pkd2 regulate extracellular matrix formation. Dis. Model. Mech. *3*, 354–365.

Miller, M.M., Iglesias, D.M., Zhang, Z., Corsini, R., Chu, L., Murawski, I., Gupta, I., Somlo, S., Germino, G.G., and Goodyer, P.R. (2011). T-cell factor/β-catenin activity is suppressed in two different models of autosomal dominant polycystic kidney disease. Kidney Int. *80*, 146–153.

Ohoka, N., Hattori, T., Kitagawa, M., Onozaki, K., and Hayashi, H. (2007). Critical and functional regulation of CHOP (C/EBP homologous protein) through the N-terminal portion. J. Biol. Chem. *282*, 35687–35694.

Oyadomari, S., and Mori, M. (2004). Roles of CHOP/GADD153 in endoplasmic reticulum stress. Cell Death Differ. *11*, 381–389.

Parnell, S.C., Magenheimer, B.S., Maser, R.L., Zien, C.A., Frischauf, A.M., and Calvet, J.P. (2002). Polycystin-1 activation of c-Jun N-terminal kinase and AP-1 is mediated by heterotrimeric G proteins. J. Biol. Chem. *277*, 19566–19572.

Qian, F., Germino, F.J., Cai, Y., Zhang, X., Somlo, S., and Germino, G.G. (1997). PKD1 interacts with PKD2 through a probable coiled-coil domain. Nat. Genet. *16*, 179–183.

Qian, F., Boletta, A., Bhunia, A.K., Xu, H., Liu, L., Ahrabi, A.K., Watnick, T.J., Zhou, F., and Germino, G.G. (2002). Cleavage of polycystin-1 requires the receptor for egg jelly domain and is disrupted by human autosomal-dominant polycystic kidney disease 1-associated mutations. Proc. Natl. Acad. Sci. USA *99*, 16981–16986.

Qian, C.N., Knol, J., Igarashi, P., Lin, F., Zylstra, U., Teh, B.T., and Williams, B.O. (2005). Cystic renal neoplasia following conditional inactivation of apc in mouse renal tubular epithelium. J. Biol. Chem. *280*, 3938–3945.

Rossetti, S., Consugar, M.B., Chapman, A.B., Torres, V.E., Guay-Woodford, L.M., Grantham, J.J., Bennett, W.M., Meyers, C.M., Walker, D.L., Bae, K., et al; CRISP Consortium. (2007). Comprehensive molecular diagnostics in autosomal dominant polycystic kidney disease. J. Am. Soc. Nephrol. *18*, 2143–2160.

Saadi-Kheddouci, S., Berrebi, D., Romagnolo, B., Cluzeaud, F., Peuchmaur, M., Kahn, A., Vandewalle, A., and Perret, C. (2001). Early development of polycystic kidney disease in transgenic mice expressing an activated mutant of the beta-catenin gene. Oncogene *20*, 5972–5981.

Shearman, M.S., Beher, D., Clarke, E.E., Lewis, H.D., Harrison, T., Hunt, P., Nadin, A., Smith, A.L., Stevenson, G., and Castro, J.L. (2000). L-685,458, an aspartyl protease transition state mimic, is a potent inhibitor of amyloid beta-protein precursor gamma-secretase activity. Biochemistry *39*, 8698–8704.

Shibazaki, S., Yu, Z., Nishio, S., Tian, X., Thomson, R.B., Mitobe, M., Louvi, A., Velazquez, H., Ishibe, S., Cantley, L.G., et al. (2008). Cyst formation and activation of the extracellular regulated kinase pathway after kidney specific inactivation of Pkd1. Hum. Mol. Genet. *17*, 1505–1516.

Shillingford, J.M., Murcia, N.S., Larson, C.H., Low, S.H., Hedgepeth, R., Brown, N., Flask, C.A., Novick, A.C., Goldfarb, D.A., Kramer-Zucker, A., et al. (2006). The mTOR pathway is regulated by polycystin-1, and its inhibition reverses renal cystogenesis in polycystic kidney disease. Proc. Natl. Acad. Sci. USA *103*, 5466–5471.

Starremans, P.G., Li, X., Finnerty, P.E., Guo, L., Takakura, A., Neilson, E.G., and Zhou, J. (2008). A mouse model for polycystic kidney disease through a somatic in-frame deletion in the 5′ end of Pkd1. Kidney Int. *73*, 1394–1405.

Struhl, G., and Adachi, A. (2000). Requirements for presenilin-dependent cleavage of notch and other transmembrane proteins. Mol. Cell *6*, 625–636.

Takiar, V., and Caplan, M.J. (2011). Polycystic kidney disease: pathogenesis and potential therapies. Biochim. Biophys. Acta *1812*, 1337–1343. Published online December 10, 2010. 10.1016/j.bbadis.2010.11.014.

Talbot, J.J., Shillingford, J.M., Vasanth, S., Doerr, N., Mukherjee, S., Kinter, M.T., Watnick, T., and Weimbs, T. (2011). Polycystin-1 regulates STAT activity by a dual mechanism. Proc. Natl. Acad. Sci. USA *108*, 7985–7990.

Taniguchi, Y., Kim, S.H., and Sisodia, S.S. (2003). Presenilin-dependent "gamma-secretase" processing of deleted in colorectal cancer (DCC). J. Biol. Chem. *278*, 30425–30428.

Tenev, T., Böhmer, S.A., Kaufmann, R., Frese, S., Bittorf, T., Beckers, T., and Böhmer, F.D. (2000). Perinuclear localization of the protein-tyrosine

phosphatase SHP-1 and inhibition of epidermal growth factor-stimulated STAT1/3 activation in A431 cells. Eur. J. Cell Biol. *79*, 261–271.

van de Wetering, M., Cavallo, R., Dooijes, D., van Beest, M., van Es, J., Loureiro, J., Ypma, A., Hursh, D., Jones, T., Bejsovec, A., et al. (1997). Armadillo coactivates transcription driven by the product of the Drosophila segment polarity gene dTCF. Cell *88*, 789–799.

Wilson, P.D. (2004). Polycystic kidney disease. N. Engl. J. Med. *350*, 151–164.

Woodward, O.M., Li, Y., Yu, S., Greenwell, P., Wodarczyk, C., Boletta, A., Guggino, W.B., and Qian, F. (2010). Identification of a polycystin-1 cleavage product, P100, that regulates store operated Ca entry through interactions with STIM1. PLoS One *5*, e12305.

Zhang, K., Ye, C., Zhou, Q., Zheng, R., Lv, X., Chen, Y., Hu, Z., Guo, H., Zhang, Z., Wang, Y., et al. (2007). PKD1 inhibits cancer cells migration and invasion via Wnt signaling pathway in vitro. Cell Biochem. Funct. *25*, 767–774.

Novel sensory signaling systems in the kidney

Jennifer L. Pluznick[a] *and Michael J. Caplan*[b]

Purpose of review
This review summarizes recent literature highlighting the roles of chemical and mechanical sensory receptors in renal function.

Recent findings
Both chemoreceptors and mechanoreceptors play important roles in renal physiology; here, we discuss specific examples of both chemoreceptors and mechanoreceptors in the kidney.

Summary
In order to maintain homeostasis, the kidney uses sensory receptors to assess the composition and rate of flow of the forming urine. Understanding the roles of these receptors will help us to better understand how the kidney functions both in health and in disease.

Keywords
chemoreceptor, kidney, mechanosensor, olfactory receptor

INTRODUCTION

A primary function of the kidney is to maintain homeostasis, and in order to do so it must monitor the concentration of a wide variety of substances in both the plasma and in the forming urine. The crucial role of the kidney in this process is revealed rather dramatically in the chemical consequences of renal failure, which can include hyponatremia, hyperkalemia, acidosis, uremia and volume expansion. To properly regulate acid–base balance, electrolyte balance, salt and water balance, the excretion of toxins, and many other processes, the kidney must be able to accurately monitor the concentrations of these substances. Sensory receptors would seem to be especially well adapted for this task, as they are specialized chemosensors (or mechanosensors), and they have been shown previously to play important roles in a variety of other tissues, some of which (like the kidney) are not typically thought of as sensory organs. For example, the sour taste receptor is found not only in the tongue, but also in neurons of the spinal column, wherein it plays a key role in sensing the pH of cerebrospinal fluid [1]. In addition, the tongue's bitter taste receptors are also found in airway smooth muscle and on the cilia of airway epithelial cells in the lung, wherein they mediate robust bronchodilation and increases in ciliary beat frequency, respectively, in response to certain inhalants [2▪,3]. The tongue's sweet taste receptors regulate glucose transport and neuroendocrine secretion in the small intestine [4,5], and are also expressed in the bladder [6▪]. Individual representatives of the nose's enormous complement of olfactory receptors have been reported to be expressed in muscle [7] and in sperm [8]. Often, ligands for these receptors are generated by essential physiological processes or metabolic pathways [1,9], indicating that metabolites and other chemicals serve signaling functions beyond their traditional roles [10,11▪▪,12].

In addition, the kidney must also monitor non-ligand based sensory modalities, such as flow rate, pressure and shear stress. These mechanical forces are well known to regulate acutely the activities of renal ion channels [13▪▪,14,15▪,16–20] as well as the activities of other renal effector proteins [21–24]. Fluid flow also plays a key signaling role in developmental processes such as planar cell polarity, which contribute to generating the nephron's unique architecture. A role for fluid flow in this process has been established in model organisms

[a]Department of Physiology, Johns Hopkins University School of Medicine, Baltimore, Maryland and [b]Department of Cellular and Molecular Physiology, Yale University School of Medicine, New Haven, Connecticut, USA

Correspondence to Michael J. Caplan, Department of Cellular and Molecular Physiology, 333 Cedar St., SHM B-147 Yale University School of Medicine, New Haven, CT 06520, USA. Tel: +1 203 785 7316; fax: +1 203 785 4950; e-mail: michael.caplan@yale.edu

Curr Opin Nephrol Hypertens 2012, 21:404–409
DOI:10.1097/MNH.0b013e328354a6bd

KEY POINTS

- Sensory signaling pathways are now appreciated to play important roles in 'nonsensory' tissues.
- The kidney uses chemoreceptors such as GPR91, IRR and the olfactory signaling pathway in order to monitor the composition of the plasma and/or forming urine, and to maintain homeostasis.
- The kidney utilizes mechanoreceptors, including (but not limited to) those found in the cilium, to monitor flow rate and shear stress in the renal tubule.

such as *Drosophila* [25▪], and it has been suggested that fluid flow may play a role in orienting planar cell polarity in the vertebrate kidney [26,27]. Mechanosensation, therefore, is another important sensory modality that the kidney may use in order to monitor critical homeostatic data.

Given the essential role that the kidney plays in maintaining homeostasis, the wide range of substances which that it must monitor in order to do, and the precedent of sensory receptors being used in other nonsensory tissues, it is logical to suggest that such receptors may also be playing sensory roles in the kidney. In this review, we will highlight several recent examples of the ways that chemosensory and mechanosensory pathways have been shown to play a role in the function of the kidney.

RENAL CHEMOSENSORS

There are several recent examples of chemoreceptors that play important roles in the kidney. Below we highlight recent studies that document a role for G-protein coupled receptor 91 (GPR91), the olfactory signaling pathway, and the insulin receptor-related receptor in modulating various aspects of renal homeostasis.

Succinate receptor

One class of substances that the kidney clearly employs chemosensors to monitor comprises the molecular intermediates and byproducts produced during energy metabolism. The most well developed and well studied example of this chemosensory capacity is that of the succinate receptor, GPR91. Although succinate is principally present in the mitochondria, in which it functions as part of the tricarboxylic acid (TCA) cycle, it is also found in the plasma in the μM range [10]. Intriguingly, tissue succinate levels rise in response to hypoxia, whereas the concentrations of other TCA intermediates fall [28,29]. Consequently, succinate levels can be an index of the level of oxidative stress, hypoxia, and mitochondrial stress. Recently, it was demonstrated that the succinate receptor, GPR91, is highly expressed in the kidney, and that succinate induces a GPR91-dependent hypertensive response in animals [10,30]. This response was shown to be dependent on the renin–angiotensin system [10]. Subsequent studies localized GPR91 to the macula densa, the cortical thick ascending limb, and to both the cortical and inner medullary collecting ducts [31]. The mechanism of the increase in blood pressure in response to succinate is now understood to involve succinate binding to GPR91 in the macula densa cells, which leads to renin release from the juxtaglomerular apparatus (JGA) [12]. Thus, the capacity to sense succinate levels may permit the kidney to increase systemic blood pressure and hence its own perfusion in response to renal energy deprivation.

Recent studies have also demonstrated that renal GPR91 and succinate chemosensation may contribute to disease pathogenesis. High glucose levels, such as those that develop in the STZ model of diabetes, lead to local accumulation of succinate and cause increased renin release from the renal JGA [28,32]. Increased succinate levels were also seen in the urine of diabetic mice (1–2 orders of magnitude, [32]), indicating that urine succinate levels could be a potential biomarker for detecting diabetic nephropathy early on in the disease progression. By stimulating renin release in response to the elevated succinate levels that accompany hyperglycemia, therefore, the succinate/GPR91 pathway is well situated to participate in producing the hypertension that is associated with the development of the metabolic syndrome [32].

Olfactory signaling pathway

Olfactory receptors are seven transmembrane G-protein coupled receptors that act as chemosensors in the olfactory epithelium [33]. Recent studies have shown that olfactory receptors also play important roles outside of the nose, wherein they serve as specialized chemosensors in a variety of tissues including myocytes [7] and sperm [8]. We have recently demonstrated that major components of the olfactory signaling pathway are present in the kidney, including olfactory receptors themselves as well as their obligatory downstream signaling partners, the olfactory G protein (G_{olf}) and the olfactory form of adenylate cyclase (AC3) [34]. AC3 localizes primarily to the distal convoluted tubule and to the macula densa. Mice null for AC3 expression cannot smell [35], consistent with the key role that this

protein plays in the nose. These AC3 knockout animals were found to have decreased plasma renin levels and a decreased glomerular filtration rate (GFR) [34], consistent with a perturbation in macula densa function. The decreased GFR and the localization of AC3 to the macula densa would seem to suggest that loss of AC3 leads to a dysregulation of the tubuloglomerular feedback (TGF) pathway; however, TGF (as measured by stop-flow pressure in response to varying perfusion rates of artificial tubular fluid) was normal in AC3 null animals. Importantly, however, these studies were done using an artificial perfusate whose composition was consistent with the ionic composition of tubular fluid, but that was likely missing many other aspects of native tubular fluid (i.e., small filtered proteins, peptides, hormones, or other metabolites). Because the ligand for this AC3-dependent pathway is unknown, it is not possible to rule out the possibility that the AC3 wild-type and null mice appeared to have similar TGF responses only because the physiological ligand was absent. Although the details of the physiological response may not yet be fully understood, it is clear that the olfactory signaling pathway plays an important physiological role in the kidney. Future studies will be required to delineate the renal 'olfactory' system's downstream signaling pathways, to identify the ligands for individual renal olfactory receptors, and to relate the renal olfactory machinery to specific physiological functions.

Insulin receptor-related receptor

Recent work by Deyev *et al.* [36▪▪] has demonstrated a role for the insulin receptor-related receptor (IRR) in acid–base balance. Careful work to identify a ligand for IRR (which was, at the time, considered an orphan receptor) led to the finding that this receptor is activated by mildly alkaline extracellular pH. This was especially surprising given that the IRR has two close homologues which both are activated by peptides [37]. Consistent with a potential role in acid–base balance, the authors found that the IRR is expressed primarily in the β-type intercalated cells of the renal distal nephron (which play a key role in acid–base balance). These studies further demonstrated that the IRR is necessary for a proper response to alkali loading. Mice that lack IRR expression are not able to increase urinary HCO_3 excretion in response to an initial alkali load, resulting in compensated metabolic alkalosis. Therefore, it appears that the IRR may play a novel role in the kidney as an alkali sensor, which acts to help manage excess bicarbonate.

RENAL MECHANOSENSORS

The concentrations of chemical compounds constitute only one variety of signals which renal epithelial cells are capable of monitoring. Numerous mechanisms are brought to bear in order to keep track of the rate of fluid flow through the nephron. Information acquired by renal mechanosensors critically influences transport processes throughout the nephron.

The cilium and mechanosensation

Just over 10 years ago [38,39] the seminal work of Praetorius and Spring established that the primary cilium can serve as a mechanosensitive organelle. The primary cilium is characterized by a '9 + 0' arrangement of microtubules in its central axoneme, in contrast to the '9 + 2' arrangement that is found in motile cilia such as those that grace the apical surfaces of airway epithelial cells. Because they lack a central pair of microtubules, primary cilia are nonmotile, and appear to serve an entirely sensory function. What they lack in motility, however, primary cilia make up for in ubiquity. Primary cilia are found on many, if not most, cell types in essentially every tissue, and they come in a variety of shapes and sizes. The photosensitive outer segment of retinal rod cells, for example, is a highly specialized primary cilium. Clusters of primary cilia adorning the apical surfaces of olfactory sensory neurons protrude into the air space of the nose and carry within their membranes the G protein coupled olfactory receptors that permit us to interrogate the chemical composition of our environment. Praetorius *et al.* [39] showed that bending the primary cilium of renal epithelial cells, either directly or via fluid flow, led to increases in cytosolic calcium levels and the opening of calcium-sensitive potassium channels. Elimination of the cilium, either chemically or genetically, blocked the flow-induced increase in cytosolic calcium [40,41]. In the renal distal nephron, flow stimulates the large-conductance Ca^{2+}-activated K^+ channel by initiating a calcium-dependent process, which ultimately leads to an increase in potassium excretion [20,42–44].

A number of studies suggest that bending the primary cilium can also activate a variety of additional signaling pathways. In intact medullary thick ascending limbs, fluid flow induces ATP release [45,46]. This nucleotide release occurs at both apical and basolateral surfaces and appears to be mediated by connexin 30 hemichannels. The released ATP activates apical and basolateral purinergic receptors, and impairing the capacity of these receptors to detect the released ATP blocks flow-induced elevations in intracellular calcium concentrations. Activating the apical P2Y2 receptor

inhibits tubular sodium transport [47]. Finally, in addition to flow, pressure pulses can induce ATP release by cultured renal epithelial cells. This pressure-induced nucleotide release appears to be independent of the cilium [48]. The molecular nature of the mechanosensitive machinery that operates within the primary cilium remains to be fully elucidated. A large body of evidence, however, indicates that the polycystin proteins contribute to this capability. Autosomal dominant polycystic kidney disease is caused by mutations in the genes encoding polycystin-1 and polycystin-2. Polycystin-1 is an extremely large protein, which is thought to span the membrane 11 times. Polycystin-2 is a member of the transient receptor potential (TRP) family of cation channels. Many TRP channel family members serve as receptors for a variety of sensory stimuli. Polycystin-1 and polycystin-2 interact with one another through their C terminal tails and this protein complex accumulates at the primary cilium [49]. Bending the primary cilium appears to activate the calcium-permeable cation channel activity of polycystin-2 [50]. The capacity of the polycystin complex to manifest this flow sensitive channel activity appears to require the functional participation of TRPV4, another member of the TRP family [51]. In the absence of fluid flow, the polycystins send a very different type of message. Perturbations of renal tubular fluid flow initiate proteolytic cleavages that release portions of the polycystin-1C terminal tail, which enters the nucleus and can modulate the activities of transcription factors [23,52▪▪,53,54].

In addition to possessing its own intrinsic flow-activated channel activity, the polycystin-1 and 2 complex is capable of regulating the activities of stretch-activated ion channels that participate in pressure sensing. When expressed alone, polycystin-2 inhibits the activities of these stretch-activated channels, whereas coexpression with polycystin-1 relieves this inhibition. On the basis of these observations, it has been suggested that the relative expression levels of polycystin-1 and 2 determine the sensitivity of a cell's complement of stretch-activated channels to pressure stimuli [55].

Fluid flow in the regulation of intercalated cell transport

Recent studies demonstrate that shear stress plays a role in transport and volume regulation in renal intercalated cells and in a culture model of this cell type (C11-MDCK cells, [56,57]). For example, using intracellular pH-sensitive fluorescent dyes to monitor proton efflux, it has been shown that fluid flow in the renal collecting duct stimulates the activity of H^+-ATPase [58]. Thus, flow is able to stimulate acid secretion into the tubule lumen. In addition, the large-conductance, Ca^{2+}-activated K^+ channel (BK) is natively expressed in renal intercalated cells, in which it is composed of both the α and the β4 subunit proteins [59]; the same subunit composition is found in C11-MDCK [16]. This apical BK-α/β4 acts as a regulator of cell volume in response to changes in shear stress [16]. An increase in shear stress leads both to a decrease in cell volume, and to K^+ efflux, which is dependent on the presence of BK-β4. Although flow sensing in the renal tubular lumen is generally thought to be the provence of cilia, interestingly, intercalated cells are one of the few cell types in the body which appear to not be ciliated. It is noteworthy, however, that the apical surfaces of type A intercalated cells protrude into the tubule lumen and have numerous microvilli, and it has been proposed that bending of the microvilli may be a potential mechanism through which flow can be sensed [16,60]. A subsequent study demonstrated that the shear stress-induced K^+ efflux is dependent on ATP release and is blocked by the purinergic receptor antagonist suramin [15▪]. As noted in the preceding section, mechanical stimuli can induce ATP release from renal tubule epithelial cells and this effect is detected with MDCK cells as well [61]. Taken together, these studies suggest an intriguing new pathway by which changes in shear stress can regulate cell volume, and consequently modulate lumen diameter. Alterations in lumen diameter will influence hydraulic resistance and the volume of tubular fluid flow, which in turn helps to determine the K^+ secretory gradient [15▪].

TRPV4 as a mechanosensor

TRP proteins are known to play important roles in many aspects of sensory physiology [62], and the TRPV subfamily is known to participate in both mechanosensation and osmoregulation [14,63]. TRPV4 is expressed in the cortical collecting duct (CCD) on the apical surfaces of principal cells and in a less polarized distribution in intercalated cells [13▪▪]. Cell culture experiments that examined both native and transfected TRPV4 demonstrated that TRPV4 acts both as a mechanosensor (necessary for calcium influx in response to increased flow/shear stress), as well as an osmosensor (necessary for calcium influx in response to hypotonicity) [64]. Thus, TRPV4 is an example of a renal protein that appears to act both as a mechanosensor and as a chemosensor, highlighting the importance of both pathways in renal physiology. Subsequent studies further characterized this signaling pathway by examining the role of native TRPV4 using the

split-open tubule preparation. Using calcium imaging and a TRPV4 agonist, these experiments revealed that TRPV4 in the native tubule is both present and functional. Furthermore, luminal fluid flow was shown to cause an increase in intracellular Ca^{2+} that is absent in TRPV4 null mice and that is similarly absent in the presence of a TRPV inhibitor [13▪▪]. Ca^{2+} influx in response to flow in the CCD is necessary for physiological responses such as flow-induced K^+ secretion [42], and therefore flow-induced changes in cytosolic Ca^{2+} levels can exert an important effect on potassium homeostasis. Although the TRPV subfamily members in general are thought to be mechanosensitive [14,63], recent studies have implied that perhaps TRPV4 may serve as a transducer of mechanical stimuli rather than a sensor [65–69]. Future studies will be required to carefully determine the nature of the components that participate in this important mechanosensitive pathway.

CONCLUSION

The molecular machinery and signaling pathways that operate in what are thought of as classical sensory organs have come to be appreciated as important regulators of functions outside traditional 'sensory' tissues, including the cerebrospinal fluid [1], muscle [7], lung [2▪,3], bladder [6▪], and sperm [8]. Recent studies demonstrate that sensory signaling pathways also play important roles in the kidney, and that these pathways involve both chemosensation and mechanosensation. Future studies will continue to uncover and further define these pathways and their roles in regulating renal physiology.

Acknowledgements

We wish to acknowledge all members of the Pluznick and Caplan laboratories who have contributed to our efforts to understand renal signaling mechanisms. This work was supported by NIH ROO DK081610 (JLP) and NIHDK090744, DoD CDMRP PR093488 and the Leducq Foundation (MJC).

Conflicts of interest

There are no conflicts of interest.

REFERENCES AND RECOMMENDED READING

Articles of particular interest, published within the annual period of review, have been highlighted as:

- ▪ of special interest
- ▪▪ of outstanding interest

Additional references related to this topic can also be found in the Current World Literature section in this issue (p. 454).

1. Huang AL, Chen X, Hoon MA, *et al.* The cells and logic for mammalian sour taste detection. Nature 2006; 442:934–938.
2. ▪ Deshpande DA, Wang WC, McIlmoyle EL, *et al.* Bitter taste receptors on airway smooth muscle bronchodilate by localized calcium signaling and reverse obstruction. Nat Med 2010; 16:1299–1304.

Inhalation of bitter tastants cause relaxation of airway smooth muscle via activation of bitter taste receptors in the lung.

3. Shah AS, Ben-Shahar Y, Moninger TO, *et al.* Motile cilia of human airway epithelia are chemosensory. Science 2009; 325:1131–1134.
4. Jang HJ, Kokrashvili Z, Theodorakis MJ, *et al.* Gut-expressed gustducin and taste receptors regulate secretion of glucagon-like peptide-1. Proc Natl Acad Sci U S A 2007; 104:15069–15074.
5. Margolskee RF, Dyer J, Kokrashvili Z, *et al.* T1R3 and gustducin in gut sense sugars to regulate expression of Na^+-glucose cotransporter 1. Proc Natl Acad Sci U S A 2007; 104:15075–15080.
6. ▪ Elliott RA, Kapoor S, Tincello DG. Expression and distribution of the sweet taste receptor isoforms T1R2 and T1R3 in human and rat bladders. J Urol 2011; 186:2455–2462.

The same receptors that detect sweet taste on the tongue appear to be expressed in the bladder, wherein they may participate in modulating bladder contractility.

7. Griffin CA, Kafadar KA, Pavlath GK. MOR23 promotes muscle regeneration and regulates cell adhesion and migration. Dev Cell 2009; 17:649–661.
8. Spehr M, Gisselmann G, Poplawski A, *et al.* Identification of a testicular odorant receptor mediating human sperm chemotaxis. Science 2003; 299:2054–2058.
9. Magistroni R, Furci L, Albertazzi A. Autosomal dominant polycystic kidney disease: from genes to cilium. G Ital Nefrol 2008; 25:183–191.
10. He W, Miao FJ, Lin DC, *et al.* Citric acid cycle intermediates as ligands for orphan G-protein-coupled receptors. Nature 2004; 429:188–193.
11. ▪▪ Kimura I, Inoue D, Maeda T, *et al.* Short-chain fatty acids and ketones directly regulate sympathetic nervous system via G protein-coupled receptor 41 (GPR41). Proc Natl Acad Sci U S A 2011; 108:8030–8035.

This article provides evidence suggesting that short chain fatty acids, which are produced primarily by commensal bacteria in the gut and absorbed by the colonic epithelium, can act as signaling molecules that exert profound effects on the activity of the autonomic nervous system.

12. Vargas SL, Toma I, Kang JJ, *et al.* Activation of the succinate receptor GPR91 in macula densa cells causes renin release. J Am Soc Nephrol 2009; 20:1002–1011.
13. ▪▪ Berrout J, Jin M, Mamenko M, *et al.* Function of TRPV4 as a mechanical transducer in flow-sensitive segments of the renal collecting duct system. J Biol Chem 2012; 287:8782–8791.

This study demonstrates that TRPV4 asks as a sensor and/or transducer of flow-induced mechanical stress in split-open tubule preperations from the renal distal nephron.

14. O'Neil RG, Heller S. The mechanosensitive nature of TRPV channels. Pflugers Arch 2005; 451:193–203.
15. ▪ Holtzclaw JD, Cornelius RJ, Hatcher LI, Sansom SC. Coupled ATP and potassium efflux from intercalated cells. Am J Physiol Renal Physiol 2011; 300:F1319–F1326.

Shear stress-induced K^+ efflux is shown to be dependent both on purinergic signaling and on BK-α/β4.

16. Holtzclaw JD, Liu L, Grimm PR, Sansom SC. Shear stress-induced volume decrease in C11-MDCK cells by BK-alpha/beta4. Am J Physiol Renal Physiol 2010; 299:F507–F516.
17. Liu W, Xu S, Woda C, *et al.* Effect of flow and stretch on the $[Ca^{2+}]$i response of principal and intercalated cells in cortical collecting duct. Am J Physiol Renal Physiol 2003; 285:F998–F1012.
18. Satlin LM, Sheng S, Woda CB, Kleyman TR. Epithelial Na(+) channels are regulated by flow. Am J Physiol Renal Physiol 2001; 280:F1010–F1018.
19. Woda CB, Bragin A, Kleyman TR, Satlin LM. Flow-dependent K+ secretion in the cortical collecting duct is mediated by a maxi-K channel. Am J Physiol Renal Physiol 2001; 280:F786–F793.
20. Pluznick JL, Wei P, Grimm PR, Sansom SC. The BK-{beta}1 subunit: immunolocalization in the mammalian connecting tubule and its role in the kaliuretic response to volume expansion. Am J Physiol Renal Physiol 2005; 288:F846–F854.
21. Ortiz PA, Hong NJ, Garvin JL. Luminal flow induces eNOS activation and translocation in the rat thick ascending limb II: role of PI3 kinase and Hsp90. Am J Physiol Renal Physiol 2004; 287:F281–F288.
22. Ortiz PA, Hong NJ, Garvin JL. Luminal flow induces eNOS activation and translocation in the rat thick ascending limb I. Am J Physiol Renal Physiol 2004; 287:F274–F280.
23. Chauvet V, Tian X, Husson H, *et al.* Mechanical stimuli induce cleavage and nuclear translocation of the polycystin-1C terminus. J Clin Invest 2004; 114:1433–1443.
24. Weinbaum S, Duan Y, Satlin LM, *et al.* Mechanotransduction in the renal tubule. Am J Physiol Renal Physiol 2010; 299:F1220–F1236.
25. ▪ Aigouy B, Farhadifar R, Staple DB, *et al.* Cell flow reorients the axis of planar polarity in the wing epithelium of Drosophila. Cell 2010; 142:773–786.

This article provides an interesting experimental and theoretical exploration of the mechanisms through which physical forces such as fluid flow can be transduced to modulate epithelial morphogenesis.

26. Fischer E, Legue E, Doyen A, *et al.* Defective planar cell polarity in polycystic kidney disease. Nat Genet 2006; 38:21–23.

27. Kramer-Zucker AG, Olale F, Haycraft CJ, *et al.* Cilia-driven fluid flow in the zebrafish pronephros, brain and Kupffer's vesicle is required for normal organogenesis. Development 2005; 132:1907–1921.

28. Peti-Peterdi J. High glucose and renin release: the role of succinate and GPR91. Kidney Int 2010; 78:1214–1217.

29. Goldberg ND, Passonneau JV, Lowry OH. Effects of changes in brain metabolism on the levels of citric acid cycle intermediates. J Biol Chem 1966; 241:3997–4003.

30. Hebert SC. Physiology: orphan detectors of metabolism. Nature 2004; 429:143–145.

31. Robben JH, Fenton RA, Vargas SL, *et al.* Localization of the succinate receptor in the distal nephron and its signaling in polarized MDCK cells. Kidney Int 2009; 76:1258–1267.

32. Toma I, Kang JJ, Sipos A, *et al.* Succinate receptor GPR91 provides a direct link between high glucose levels and renin release in murine and rabbit kidney. J Clin Invest 2008; 118:2526–2534.

33. Buck L, Axel R. A novel multigene family may encode odorant receptors: a molecular basis for odor recognition. Cell 1991; 65:175–187.

34. Pluznick JL, Zou DJ, Zhang X, *et al.* Functional expression of the olfactory signaling system in the kidney. Proc Natl Acad Sci U S A 2009; 106:2059–2064.

35. Wong ST, Trinh K, Hacker B, *et al.* Disruption of the type III adenylyl cyclase gene leads to peripheral and behavioral anosmia in transgenic mice. Neuron 2000; 27:487–497.

36. ■■ Deyev IE, Sohet F, Vassilenko KP, *et al.* Insulin receptor-related receptor as an extracellular alkali sensor. Cell Metab 2011; 13:679–689.
IRR is shown to be a pH sensor in the intercalated cells of the renal distal nephron, wherein it is required for a proper renal response to alkali loading.

37. Shier P, Watt VM. Primary structure of a putative receptor for a ligand of the insulin family. J Biol Chem 1989; 264:14605–14608.

38. Praetorius HA, Spring KR. Bending the MDCK cell primary cilium increases intracellular calcium. J Membr Biol 2001; 184:71–79.

39. Praetorius HA, Frokiaer J, Nielsen S, Spring KR. Bending the primary cilium opens Ca2+-sensitive intermediate-conductance K+ channels in MDCK cells. J Membr Biol 2003; 191:193–200.

40. Praetorius HA, Spring KR. Removal of the MDCK cell primary cilium abolishes flow sensing. J Membr Biol 2003; 191:69–76.

41. Liu W, Murcia NS, Duan Y, *et al.* Mechanoregulation of intracellular Ca2+ concentration is attenuated in collecting duct of monocilium-impaired orpk mice. Am J Physiol Renal Physiol 2005; 289:F978–F988.

42. Liu W, Morimoto T, Woda C, *et al.* Ca^{2+} dependence of flow-stimulated K secretion in the mammalian cortical collecting duct. Am J Physiol Renal Physiol 2007; 293:F227–F235.

43. Liu W, Wei Y, Sun P, *et al.* Mechanoregulation of BK channel activity in the mammalian cortical collecting duct: role of protein kinases A and C. Am J Physiol Renal Physiol 2009; 297:F904–F915.

44. Rieg T, Vallon V, Sausbier M, *et al.* The role of the BK channel in potassium homeostasis and flow-induced renal potassium excretion. Kidney Int 2007; 72:566–573.

45. Jensen ME, Odgaard E, Christensen MH, *et al.* Flow-induced $[Ca^{2+}]$i increase depends on nucleotide release and subsequent purinergic signaling in the intact nephron. J Am Soc Nephrol 2007; 18:2062–2070.

46. Hovater MB, Olteanu D, Hanson EL, *et al.* Loss of apical monocilia on collecting duct principal cells impairs ATP secretion across the apical cell surface and ATP-dependent and flow-induced calcium signals. Purinergic Signal 2008; 4:155–170.

47. Leipziger J. Luminal nucleotides are tonic inhibitors of renal tubular transport. Curr Opin Nephrol Hypertens 2011; 20:518–522.

48. Praetorius HA, Frokiaer J, Leipziger J. Transepithelial pressure pulses induce nucleotide release in polarized MDCK cells. Am J Physiol Renal Physiol 2005; 288:F133–F141.

49. Chapin HC, Caplan MJ. The cell biology of polycystic kidney disease. J Cell Biol 2010; 191:701–710.

50. Nauli SM, Alenghat FJ, Luo Y, *et al.* Polycystins 1 and 2 mediate mechanosensation in the primary cilium of kidney cells. Nat Genet 2003; 33:129–137.

51. Kottgen M, Buchholz B, Garcia-Gonzalez MA, *et al.* TRPP2 and TRPV4 form a polymodal sensory channel complex. J Cell Biol 2008; 182:437–447.

52. ■■ Merrick D, Chapin H, Baggs JE, *et al.* The gamma-secretase cleavage product of polycystin-1 regulates TCF and CHOP-mediated transcriptional activation through a p300-dependent mechanism. Dev Cell 2012; 22:197–210.
This article demonstrates that a proteolytic product of the polycystin-1 protein, which is cleaved in response to changes in renal flow, modulates transcriptional pathways that may be involved in the pathogenesis of polycystic kidney disease.

53. Low SH, Vasanth S, Larson CH, *et al.* Polycystin-1, STAT6, and P100 function in a pathway that transduces ciliary mechanosensation and is activated in polycystic kidney disease. Dev Cell 2006; 10:57–69.

54. Talbot JJ, Shillingford JM, Vasanth S, *et al.* Polycystin-1 regulates STAT activity by a dual mechanism. Proc Natl Acad Sci U S A 2011; 108: 7985–7990.

55. Sharif-Naeini R, Folgering JH, Bichet D, *et al.* Polycystin-1 and -2 dosage regulates pressure sensing. Cell 2009; 139:587–596.

56. Gekle M, Wunsch S, Oberleithner H, Silbernagl S. Characterization of two MDCK-cell subtypes as a model system to study principal cell and intercalated cell properties. Pflugers Arch 1994; 428:157–162.

57. Wunsch S, Gekle M, Kersting U, *et al.* Phenotypically and karyotypically distinct Madin-Darby canine kidney cell clones respond differently to alkaline stress. J Cell Physiol 1995; 164:164–171.

58. Liu W, Pastor-Soler NM, Schreck C, *et al.* Luminal flow modulates H+-ATPase activity in the cortical collecting duct (CCD). Am J Physiol Renal Physiol 2012; 302:F205–F215.

59. Grimm PR, Foutz RM, Brenner R, Sansom SC. Identification and localization of BK-beta subunits in the distal nephron of the mouse kidney. Am J Physiol Renal Physiol 2007; 293:F350–F359.

60. Wang T. Flow-activated transport events along the nephron. Curr Opin Nephrol Hypertens 2006; 15:530–536.

61. Ostrom RS, Gregorian C, Insel PA. Cellular release of and response to ATP as key determinants of the set-point of signal transduction pathways. J Biol Chem 2000; 275:11735–11739.

62. Montell C. Physiology, phylogeny, and functions of the TRP superfamily of cation channels. Sci STKE 2001; 2001:re1.

63. Liedtke WB. TRPV channels' function in osmo- and mechanotransduction. In: Liedtke WB, Heller S, editors. Source TRP ion channel function in sensory transduction and cellular signaling cascades. Boca Raton, FL: CRC Press; 2007. Ch. 22.

64. Wu L, Gao X, Brown RC, *et al.* Dual role of the TRPV4 channel as a sensor of flow and osmolality in renal epithelial cells. Am J Physiol Renal Physiol 2007; 293:F1699–F1713.

65. Gao X, Wu L, O'Neil RG. Temperature-modulated diversity of TRPV4 channel gating: activation by physical stresses and phorbol ester derivatives through protein kinase C-dependent and -independent pathways. J Biol Chem 2003; 278:27129–27137.

66. Vriens J, Watanabe H, Janssens A, *et al.* Cell swelling, heat, and chemical agonists use distinct pathways for the activation of the cation channel TRPV4. Proc Natl Acad Sci U S A 2004; 101:396–401.

67. Xu F, Satoh E, Iijima T. Protein kinase C-mediated Ca^{2+} entry in HEK 293 cells transiently expressing human TRPV4. Br J Pharmacol 2003; 140:413–421.

68. Loot AE, Popp R, Fisslthaler B, *et al.* Role of cytochrome P450-dependent transient receptor potential V4 activation in flow-induced vasodilatation. Cardiovasc Res 2008; 80:445–452.

69. Fan HC, Zhang X, McNaughton PA. Activation of the TRPV4 ion channel is enhanced by phosphorylation. J Biol Chem 2009; 284:27884–27891.